Total energy calculation for prediction and structural optimization of alloys with complex or aperiodic structure

Marek Mihalkovič

Slovak Academy of Sciences, Bratislava, Slovakia

mailto: mihalkovic@savba.sk

Disclaimer and copyright notice

Introduction

State of the art, from the viewpoint of total energy calculations:
1. d-AlCoNi, its variations Co–rich, Ni–rich. They are all high–T phases, 10-20 meV/atom above tie–plane of stable crystal structures.
2. i-AlMnPd, i-AlCuFe. Crucial role of pseudo–Mackay. Approximant energies are nearly stable **down to low temperatures.** Strong (pseudo)gaps. (But the important AlRePd case is not understood yet.. Paradoxically, *all proposed stabilization theories participate importantly: (perhaps) matching rule, configurational AND vibrational entropy, electronic Hume–Rothery like.*
3. i–CdYb. Approximants based on CCT tiling (structures consistent with Takakura et al model) are *stable down to low temperature*. It is unclear what mechanism drives formation of QC phase.
4. Frank–Kasper class, bot deca. and ico., AlMgZn, AlCuLi. Approximant structures stable. Packing rules, "tile–Hamiltonians" to be completed.
5. i-MgZnRE, d-MgZnRE. Not studied yet adequately by energetic approaches.
Diffraction–data derived models of complex alloys have never good low energy "as–given", due to the disorder–averaging effects.
FUTURE: to compare quantitatively (and correctly) with diffraction data, the average structures have to be modelled as properly weighted ensembles of states with resolved occupancy correlations.

Modelling complex atomic structures...

The grand ambition of the modelling is to predict structures without any experimental inputs. Nowadays, this is hardly possible if a complexity measured by number of independent atoms exceeds few tens (or less).

At more constraining condition (eg fixed unit cell size, composition, density) AND having good empirical potentials at hand, unbiased structure predictions are possible for up to several hundreds of atoms.

In the vast majority of the case studies I will present, the exposition of the situation is: diffraction data–refined complex structure, with moderate or even high disorder arising from spatial averaging. Our ultimate goal is to replace the average structure by ensemble of ultimately plausible, low energy individual realizations. The "experimental" average structure should be then interpreted as an average over this ensemble. The ensemble of low-energy states gives us immediate access to partition function, and entropic contribution to the free energy.

... Nowadays instruments can determine atomic positions with perhaps 10^{-5}Åaccuracy. But because of averaging effects, the meaning of these accurate positions is not easily interpreted!

DFT: feasibility for large models

DFT, VASP (G. Kresse, J. Hafner, Fürthmüller, D. Joubert)

2/1 approximants: AlMnPd (544 atoms), MgScZn/CaCd (704-712), AlMgZn (680)

"K–point" mesh convergence: memory/speed requirements scale linearly with number of K–points. The convergence on K-mesh depends greatly on the system, but also on the cell shape. For example: AlCoNi is easy to converge. Difficult case, for example: ϵ–MgPd (J. Makongo and G. Kreiner)

Pearson symbol oC1536, 766 atoms per primitive cell; nearly-ortho lattice $19.8 \times 19.8 \times 38.3$Å.

	(0,0,0)	(0.5,0.5,0.5)	(1/2,1/2,1/2)	2x2x1 mesh
energy [meV/atom]	-2.630	-2.646	-2.639	-2.638

High-symmetry models like AlMgZn are easier. 2x2x2 reciprocal mesh is represented by single K-point (not Γ). Single ionic step takes 10 hrs on quad-core Nehalem

Parallelization for several 100 atom systems – plane wave codes do not parallelize easily!

- 4 cores : efficient
- 8 cores : feasible (may need tuning hardware)
- more – needs special tuning, if possible at all. Perhaps expensive with hardware (infiniband)

Methods for optimization of alloys with complex structure

One important goal: replace (structure) ensemble averages deduced from diffraction data studies, by ensembles of configurations, EACH OF WHICH has low energy. In other words, resolve correlations in occupancies, which are burried in standard diffraction data.
Corollary: in complex structures, **occupancy correlations** are important part of the structure solution!
Why is it important? A single misplaced atom may spuriously affect any calculated property. But mainly, for complex structures with subtle "matching rules" (explain later) few misplaced atoms may entirely blurr important ordering phenomena.

- molecular dynamics
- 'lattice gas" annealing
- tempering alias replica exchange method
- transfer matrix

Energy diagrams at zero temperature

- plane-wave electronic DFT code VASP
  - *relax atomic positions*
  - *relax shape/volume of unit cell*
- evaluate enthalpies of mixing dH for each compound
- convex hull $\rightarrow$ dE (package qhull)
- sampling of possible&plausible structures
  - *observed phases: Pearson Handbook and recent literature*
  - *chemical similarity of systems*
  - *models for a particular class of compounds*
  - *mixed and fractional occupancies: supercells, role of pair potentials*

http://alloy.phys.cmu.edu : At the beginning stands our collection of $\sim$2300 crystal structures, compiled from Pearson Handbook or alternative sources into an awk-managed diffraction-data based structural database. This is then interfaced to a semi-automatic VASP setup. At the moment we performed VASP relaxations for perhaps 3000 compositions.

Mg–Zn: golden mine for CMA (several different families...)

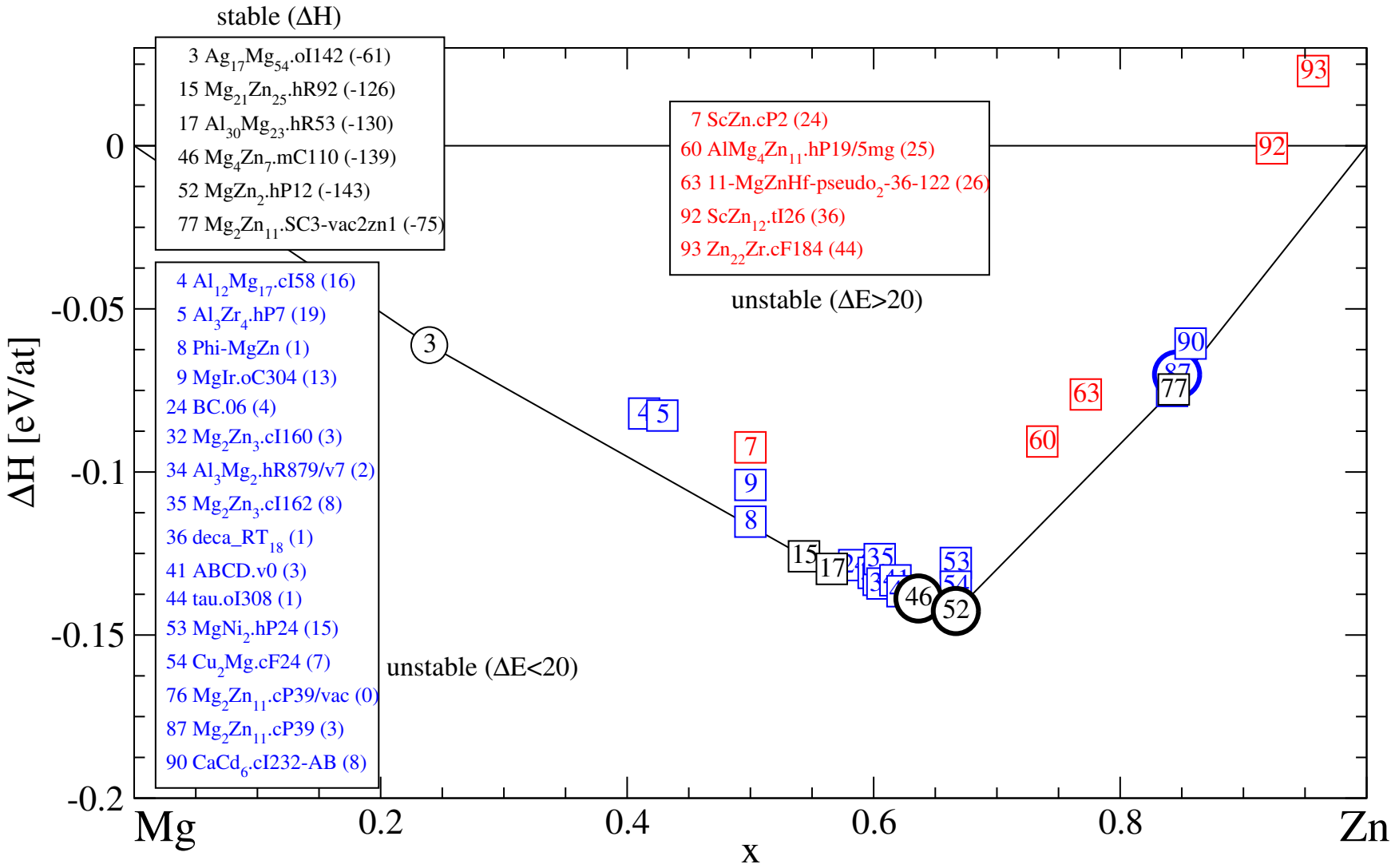

#	struc	ΔE meV/at.	ΔH meV/at.	x(Mg) %	x(Zn) %	comment
3	Ag17Mg54.oI142	-5.7	-61.1	76.1	23.9	reported high-T
52	MgZn2.hP12	-3.7	-142.6	33.3	66.7	
15	Mg21Zn25.hR92	-0.9	-125.8	45.7	54.3	
17	Al30Mg23.hR53	-0.7	-129.7	43.4	56.6	not reported
77	Mg2Zn11-SC3-v2z1.hR115	-0.2	-74.7	15.7	84.3	1/3 occup. Zn1
46	Mg4Zn7.mC110	-0.0	-138.8	36.4	63.6	decagonal app.
76	Mg2Zn11.cP39/vac	0.1	-75.2	15.8	84.2	
44	deca_τ.oI308	0.5	-136.6	37.7	62.3	reported in AlMgZn (Berthold et al)
37	deca_H2S	1.0	-134.0	39.3	60.7	
8	Φ-MgZn	1.3	-115.3	50.0	50.0	stable in ternary Al–Mg–Zn
34	Al3Mg2.hR879/v7	1.5	-133.1	39.6	60.4	stable in Al–Mg
41	ico-ABCD.v0	3.1	-133.2	38.2	61.8	more stable than pure cells!
32	ico-A.cI160	3.2	-130.9	40.0	60.0	
87	Mg2Zn11.cP39	3.3	-70.1	15.4	84.6	fully occup. clearly unstable
24	ico-BC-06.hRXX	3.5	-128.5	41.6	58.4	
90	CaCd6.cI232-AB	7.5	-60.6	14.3	85.7	CaCd6 type SLIGHTLY unstable!
54	Cu2Mg.cF24	7.5	-135.2	33.3	66.7	Laves
35	ico-A-ccfill.cI162	8.0	-126.7	39.5	60.5	
9	MgIr.oC304	12.6	-104.0	50.0	50.0	
53	MgNi2.hP24	14.7	-127.9	33.3	66.7	Laves
4	Al12Mg17.cI58	16.1	-82.1	58.6	41.4	
5	Al3Zr4.hP7	18.7	-82.7	57.1	42.9	
7	ScZn.cP2	24.1	-92.5	50.0	50.0	B2 type
60	AlMg4Zn11.hP19/5mg	25.0	-90.7	26.3	73.7	Auld et al 1978, metastable
63	11-MgZnHf-pseudo2-36-122	25.9	-76.2	22.8	77.2	stable in ternary!
92	ScZn12.tI26	35.9	-0.8	7.7	92.3	
93	Zn22Zr.cF184	43.7	22.9	4.3	95.7	

Oscillating Pair Potentials

$$V(r) = \frac{C_1}{r^{\eta_1}} + \frac{C_2}{r^{\eta_2}} \cos(k_* r + \phi_*) \tag{1}$$

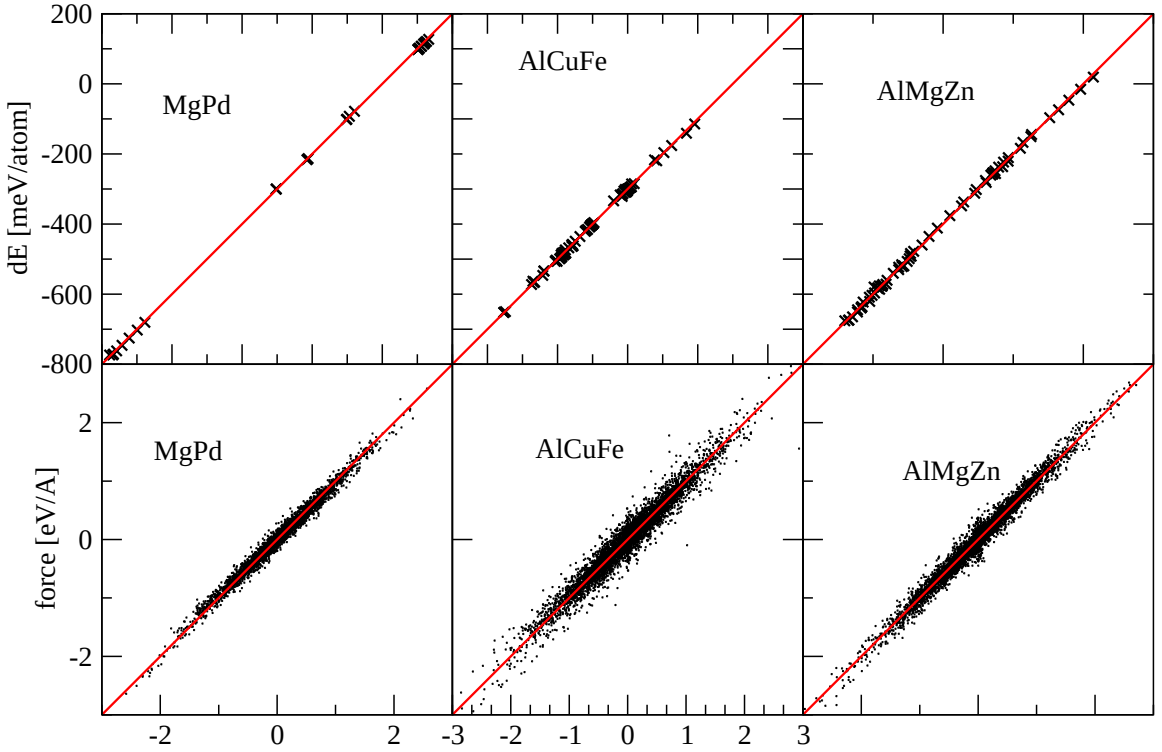

Low–temperature structure of i-AlMnPd and i-AlCuFe approximants from energetic optimization: covering by "pseudo-Mackay" clusters.

– Detailed energetic study of AlMnPd and AlCuFe ternary diagrams by ab–initio methods, including binary subsystems!

Package VASP: G. Kresse and J. Hafner, Phys. Rev. B 47, R558 (1993); G. Kresse and J. Fürthmüller, Phys. Rev. B 54, 11169 (1996); G. Kresse and D. Joubert, Phys. Rev. B 59, 1758 (1999)

– rather good oscillating pair potentials for AlCuFe, based on generalized pseudopotential theory (J. Moriarty, M. Widom et al). Rather good AlMnPd EAM potentials (D. Schopf, Stuttgart) – all fitted to VASP data

– Molecular dynamics, lattice–gas Monte Carlo, hand–modelling, analyzis, very detailed structural insight:

$\rightarrow$ new grand picture of icosahedral AlCuFe and AlMnPd: covering by pseudo–Mackay clusters, canonical-cell tiling geometry. Strikingly simple (gross picture), yes subtly complex (from local to global order)

Al-Mn-Pd energy-diagram at T=0K (VASP)

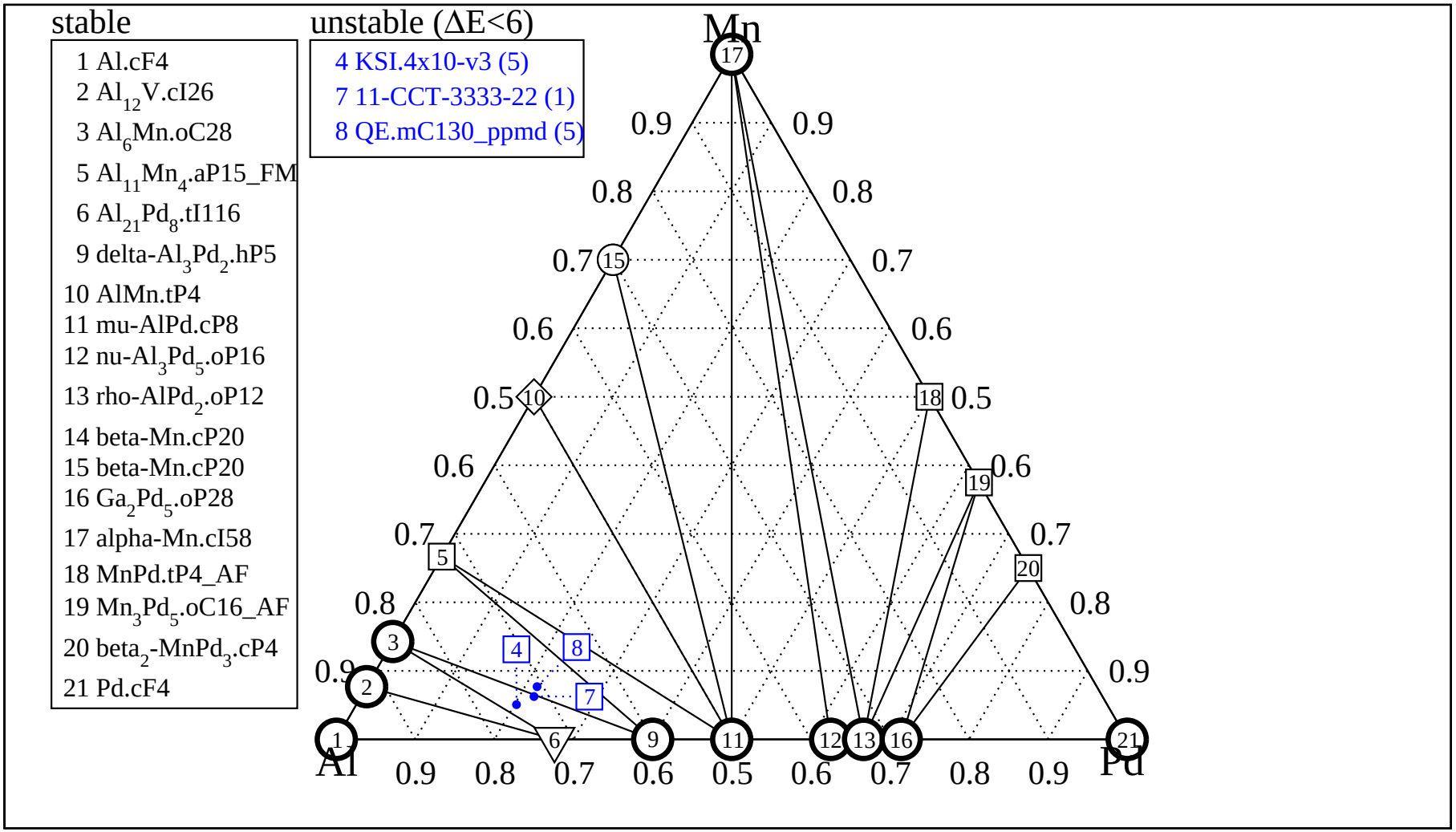

History of ab–initio refinements, AlMnPd system

How good are these models by ab–initio methods, facing competition of crystalline phases?

– 1994 ICO "KGBK" model i-AlMnPd (Katz-Gratias-Boudard-Krajci), 2/1: **+80 meV/atom**
– 2000 ICO "EQ" model (Elser-Quandt) model, RD-approximant :**+30 meV/atom**
– 2004 D16-ξ AlMnPd, Boudard diffraction + chemical order via MC-LG: **+20 meV/atom**
– 2005 ICO "EQZ" model: Zijlstra's improvement of EQ: **+14 meV/atom**
– 2006 ICO "EQZM$_2$ model: MM improvement over EQZ model: **+9 meV/atom**
– 2008 ICO "MK+MM"† 1/1 improved model (MD+quench): **+1 meV/atom**
– 2009 D16-ξ AlMnPd, A. Santana +MM pMI inner shells... **+5 meV/atom**
– 2009 D12-T AlMnPd by MK+MM - first stable ternary! - changed tie-plane!
– 2009 D16-ξ AlMnPd, B. Frigan modif. in two steps $\rightarrow$ **STABLE** ! (the best "1/1" ico. model becomes +6 meV/atom)

† Improved version of Krajci–Hafner model was obtained by (i) removing Mn-Pd nearest neighbors and using ab–initio "anneal-quench" method. After $\sim$10k MD steps and many quenches, the optimal structural energy nearly touched tie-plane!

Optimized ICO models provide fundamentally new view of the structure, which is essentaily coverings by "pseudo"-Mackay cluster.

UPDATED Al-Mn-Pd energy-diagram at T=0K (VASP)

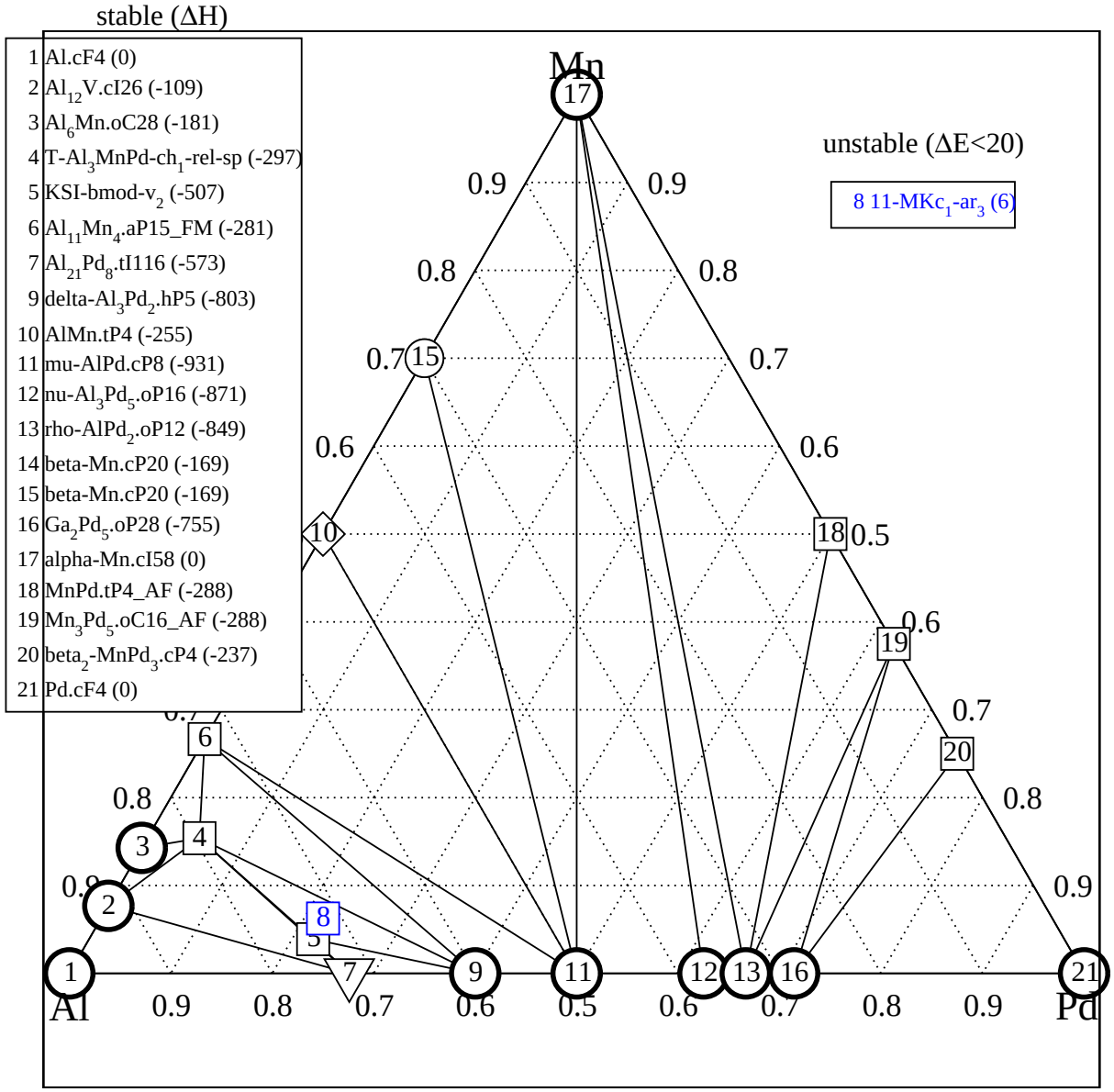

Clusters in “1/1” i-AlMnPd approximant

Al:7(+3)

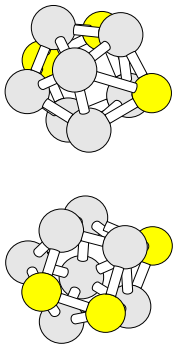

Al:27(+3), TM:12

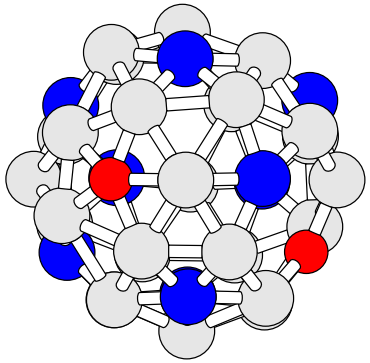

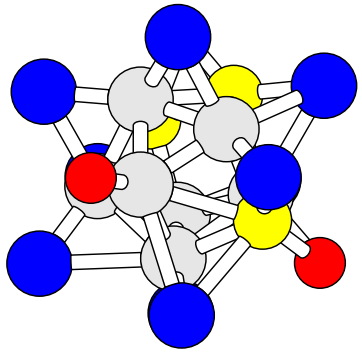

"even node"
pseudo–MI

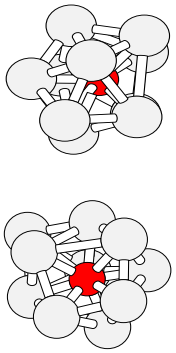

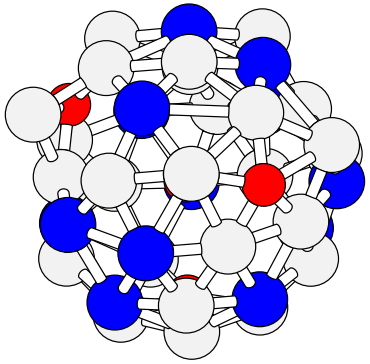

"odd node" pMI, Al:26,TM:16

"mini–Bergman"

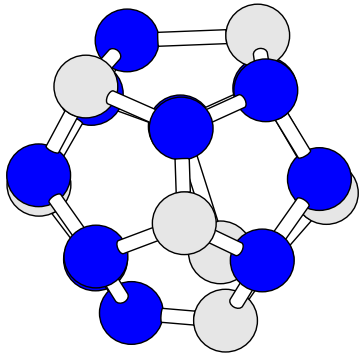

PdAl12

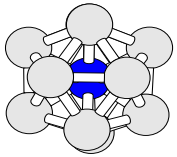

pMI clusters and Pd-centred Al_{12} are COMMON between ”D16” and ICO structures. In the 1/1 approximant, pMI cover **all** atoms, except Pd in $PdAl_{12}$ icosahedra. pMI DO HAVE unique chemical identity. Framework atoms, and “floating” Al atoms (cores).

Cluster geometry of the "1/1" approximant

Cluster centers in the optimized "1/1" approximant, space group $P2_13$, with $c{=}\tau^{-1}/4$).

vertex	X	Y	Z	cluster
A	c	c	c	pMI (Al–rich)
B	$-c$	$-c$	$-c$	ico $PdAl_{12}$
C	$0.5-c$	$0.5-c$	$0.5-c$	pMI (TM-rich)

- subset A+B : "2/1" CCT tiling (no D cells)
- subset A+C : "1/0" Penrose tiling (4 PR + 4 OR)

Canonical cell tiling (Henley, 1991)

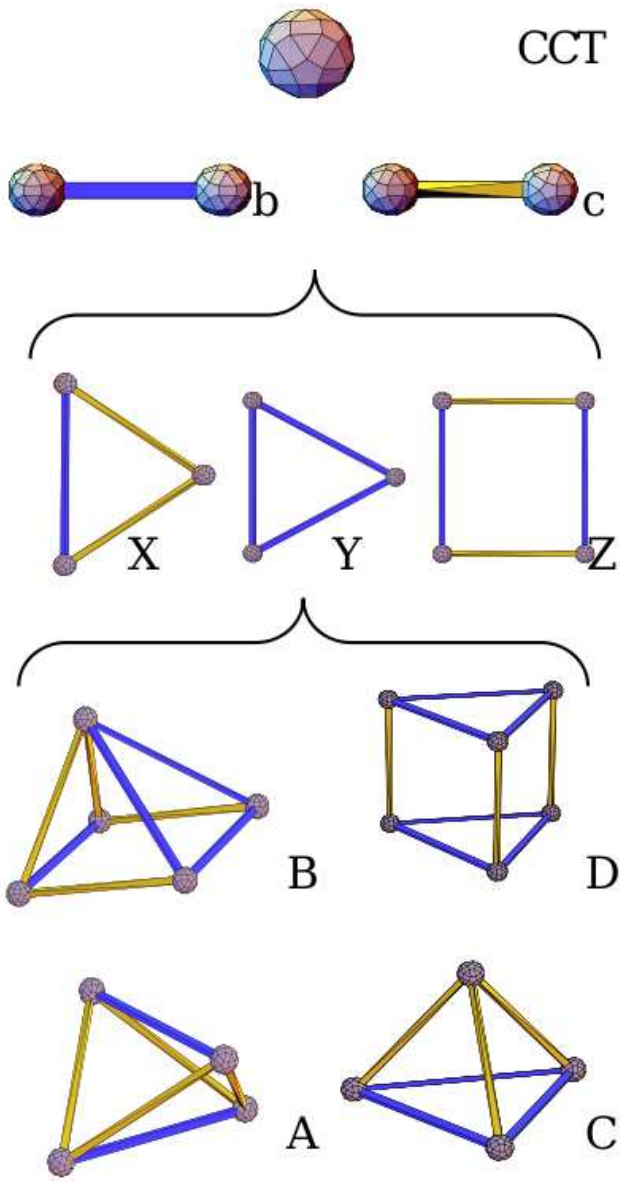

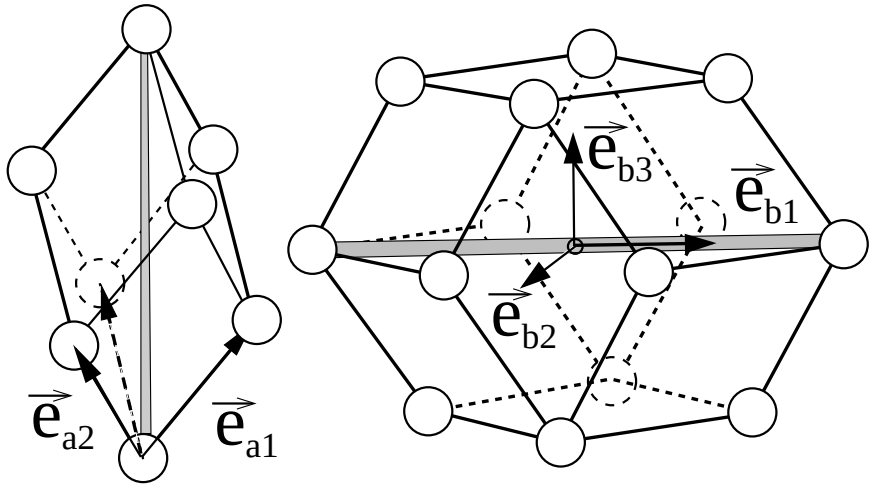

Canonical cell generalizes the BCC packing of icosahedral clusters, by finding minimal number of cells supporting formation of networks with global icosahedral symmetry. No local flip/update move. Large database of approximant tilings available.

Canonical cells decoration rule

– type-1 Mn atoms are at CCT(+) nodes
– type-2 Mn atoms are at "MI-icosahedron in Y-face" positions
– type-1 Pd atoms are at CCT(−) nodes
– type-2 Pd atoms are at "MI-icosahedron" atoms (except Mn...)
– type 1 Al atoms are pMI innermost shells: 7 Al at ∼2.4Åfrom the central Mn; 3 Al at ∼2.9Å

So far, non-deterministic feature: pseudo-MI shells.
Constraint: overlaps along 2–fold axes ("dimpling")
Connectivity along 2–fold axes: on average, each CCT node has 6 2–fold neighbors.

"Arrow rule": exhaustive search

Innermost pMI shell: we approximate the (7+3)Al atoms around Mn type 1 by:

- **2-fold linkages** (overlap! 1Al+1vac per linkage, net 3 Al per node) $\rightarrow$ "arow" associated with 2-f linkage
- **3-fold linkages** (net 7 Al per node, depending...)
- exhaustive enumeration of all possibilities: for "1/1" there are then 4096 configurations, 317 of them independent. Out of them 22 are 3333 and 40 are 2244

Ab–initio total energies of all 3333 and 2244 configurations: optimal structure exactly reproduces optimal approximant found by MD anneal-quench method! So we are farely sure this is indeed optimum!

"3333"-ARROWING VARIANTS "1/1" $P2_13$ cell, 4 pMI, PERP SPACE

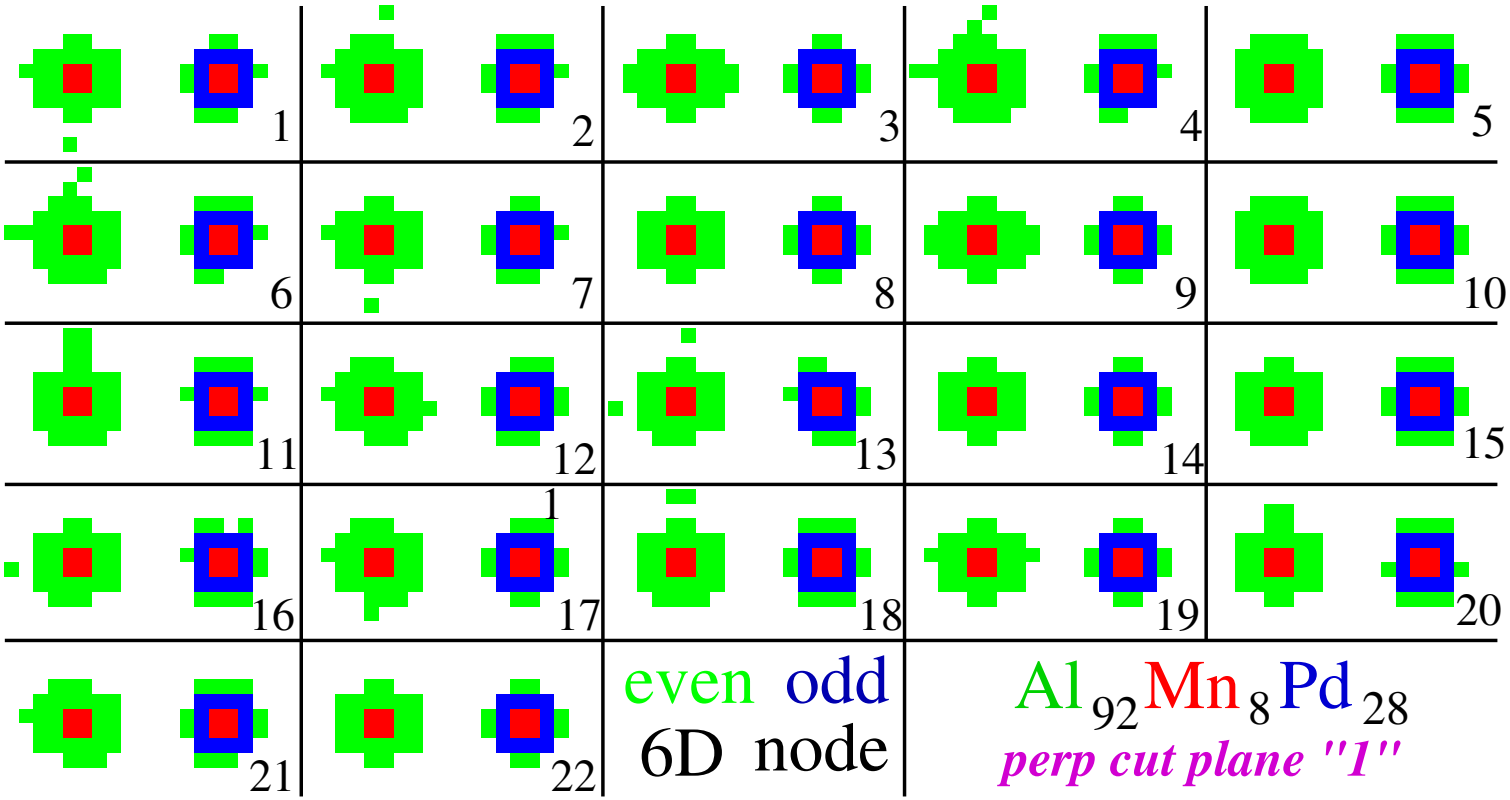

N	22	20	4	1	17	16	14	13	15	10	7	...	5
dE[eV]/cell	REF	0.33	0.67	0.67	0.70	1.02	1.02	1.10	1.16	1.19	1.48	...	6.5
dR_{max}[Å]	1.35	1.50	1.44	1.44	1.41	1.44	1.38	–	–	1.44	0.63	...	0.27

Samples 11, 13, 15 19: could not lift; energies: VASP. Notice: strikingly high energy for smallest displacement #5!

Steps towards deterministic rule, tiling Hamiltonian

- we have set up unique coding for every possible pattern of (7+3) Al

- this analyzis is *specific* to the "1/1" tiling (67-type CCT environment)! Need to extend to other environments

#	E [eV]	134	123	145	124	156	146	comment
22	REF	4	-	-	-	-		
1	0.755	2	1	1	-	-		$\rightarrow E_{123}$ ~0.36 eV
17	0.794	2	-	2	-	-		$\rightarrow E_{145}$ ~0.34 eV
16	1.101	-	1	3	-	-		$\rightarrow E_{145}$ ~0.25 eV
13	1.178	-	1	-	3	-		$\rightarrow E_{124}$ ~0.27 eV
15	1.242	1	-	-	2	1		$\rightarrow E_{156}$ ~0.70 eV
10	1.280	-	-	-	2	-	2	$\rightarrow E_{146}$ ~0.34 eV

α-AlMnSi: Proper Mackay Icosahedra are Silicon stabilized!

– T=0K VASP study. At finite temperatures, there will be important entropic term for Al/Si mixing

– X-ray diffraction alone hardly can tell the difference between Al/Si

– Three sites reported to have Si or Al/Si ocupancy experimentally (Sugiyama et al, 1998): Si (so called 6DBC position, causing even/odd symmetry breaking), M1 and M3 (small icosahedra, corner and body center)

– EOPP and Lattice Gas MC to create configurations subject to VASP calculation. Si stabilizes small MI icosahedron! 5-fold arrangement

ΔE	x_{Si}	"Si" Al,Si	"M1" Al,Si	"M3" Al,Si	comment
$\mu \rightarrow$		6	12	12	
-4.7	13.0	6,0	6,6	0,12	ch2
7.2	8.7	6,0	12,0	0,12	ch5
14.5	4.3	0,6	12,0	12,0	ch1
16.7	17.4	6,0	0,12	0,12	ch4
15.6	–	6,0	12,0	12,0	BINARY!
–	12.9	0,6	7.8,4.2	4.4,7.6	EXPE

Al/Si icosahedron.

Gray: Si, white: Al

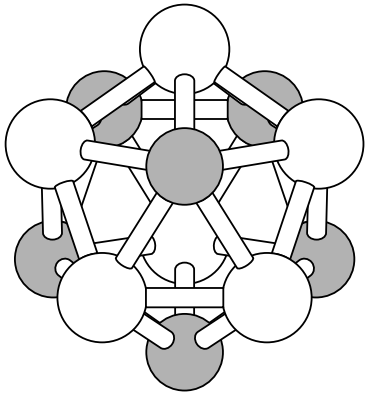

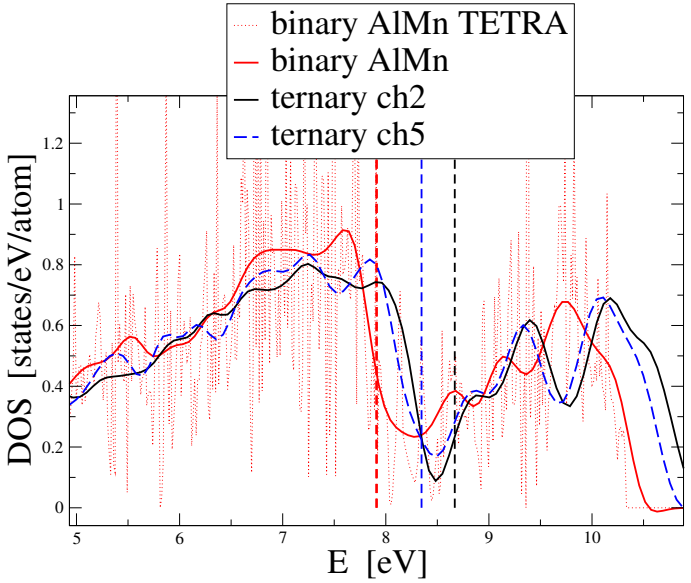

AlCuFe: combined pair–potential and DFT study

EOPP database of forces and energies: Al2Cu, Al5Fe2, Al3Fe and ω–Al7Cu2Fe, altogether 3714 force datapoints and 49 energy-difference datapoints. Final RMS for the set of forces was 0.13 eV/A, and 2.1 meV/atom for energy datapoints. Scatter plots for both classes of datapoints are shown above.

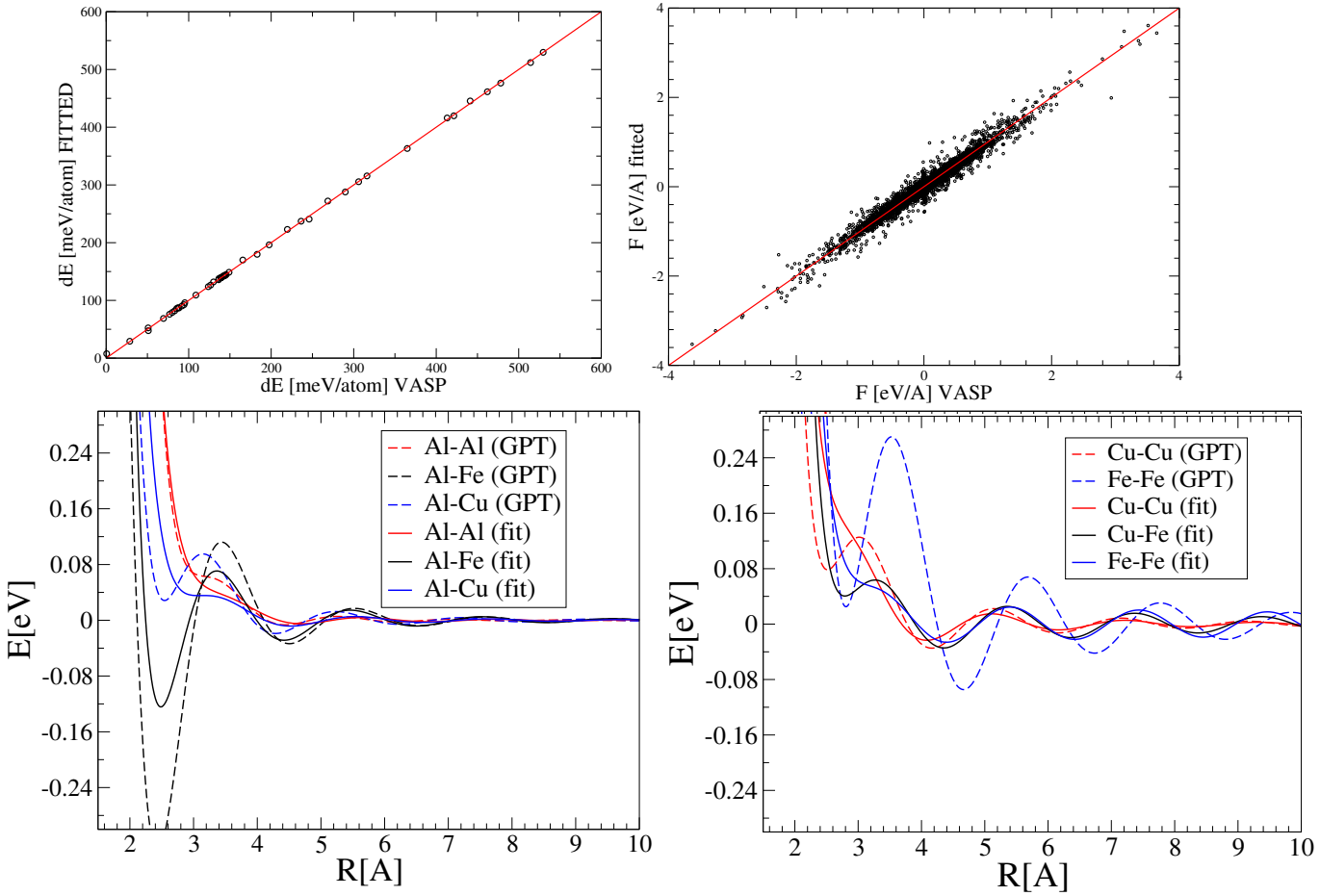

AlCuFe: optimization of icosahedral model

We used oversized (with respect to expected sizes) atomic surfaces as a fixed site list, populated by atoms in a Lattice Gas Monte Carlo annealing. FCI order develops around 3400K–2800K. The T→0 structure has connected surfaces, but low symmetry. This is enforced by minimization of rather short Al-Al distance along 3-fold axis of 2.52 A.

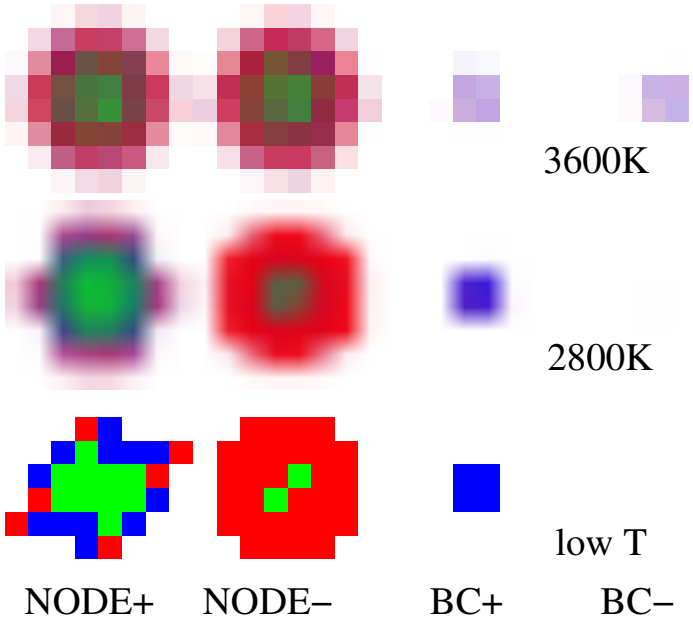

...AlCuFe: first results...

#	struc	ΔE meV/at.	ΔH meV/at.	x(Al) %	x(Cu) %	x(Fe) %
3	Al72Cu4Fe24.mC102	-4.5	-349.6	72.5	3.9	23.5
4	Al7Cu2Fe.tP40	-3.2	-270.3	70.0	20.0	10.0
7	oC28_as_Al5Fe2.ppsc	-0.1	-349.6	66.7	6.7	26.7
39	11.ch1-lgmd-temper	27.5	-263.2	62.5	25.0	12.5
37	11-CZ†	51.0	-239.6	62.5	25.0	12.5

†Improved Cockayne model, after Zijlstra et al PRB 69, 094206 (2004)

Our best model so far was **identical** to 11-CZ $\rightarrow$ our optimized potentials exactly reproduced the chemical ordering of Zijlstra et al.

After applying combined LG+MD within tempering scheme, energy decreased by 22 meV/atom – see model 11.ch1-lgmd-temper in the table

... electronic DOS, energetic stability...

After inspecting e-DOS, series of chemistry modifications. Final optimal model at +10meV/atom. This is comparable to AlMnPd icosahedral model (+7.5 meV/atom), and well within reach of entropic terms, see below.

#	struc	ΔE meV/at.	ΔH meV/at.	x(Al) %	x(Cu) %	x(Fe) %
3	Al72Cu4Fe24.mC102	-4.5	-349.6	72.5	3.9	23.5
4	Al7Cu2Fe.tP40	-3.2	-270.3	70.0	20.0	10.0
7	oC28_as_Al5Fe2.ppsc	-0.1	-349.6	66.7	6.7	26.7
15	11.ch5-lgmd-temper	10.4	-274.7	64.8	23.4	11.7
39	11.ch1-lgmd-temper	27.5	-263.2	62.5	25.0	12.5
37	11-CZ†	51.0	-239.6	62.5	25.0	12.5

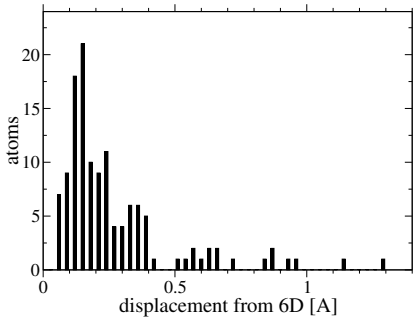

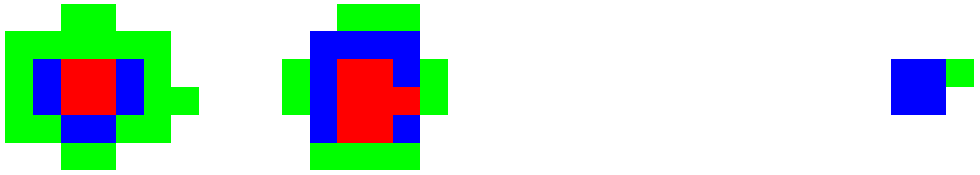

NODE+ NODE− BC+ BC−

$Al_{83}Fe_{15}Cu_{30}$ 128 atoms/cell

Electronic DOS, vibrational entropy

1. According to the EOPP-potential computed VDOS, 1/1–AlCuFe "11.ch5-lgmd-temper" model would become stable against Al7Cu2Fe tP40 crystal structure at ∼820K, and **both would coexist** at higher temperatures.

2. Electronic DOS has a deep pseudogap (almost a gap), very similar to AlMnPd. Fermi level falls in both cases just on the top of feature near the bottom of the pseudogap. Possibly, this coincidence prevents 1/1 geometry to further lower energy.

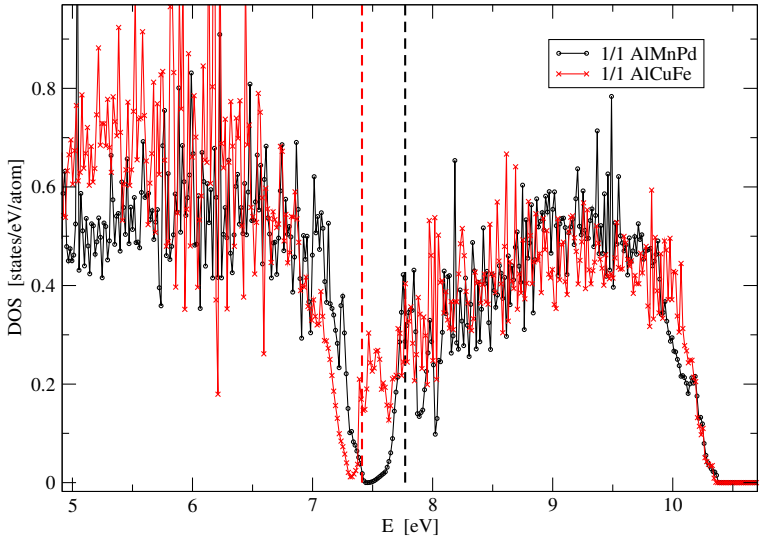

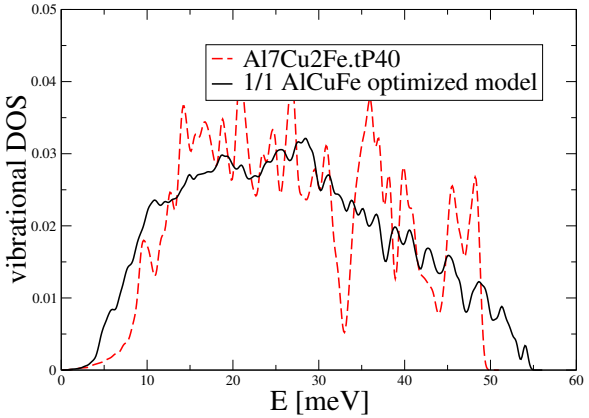

i-AlPdMn and iAlCuFe, summary

- there are definitely unique, chemically relevant clusters building/covering i-AlCuFe and i-AlMnPd structures: so-called bf pseudo–Mackay's, that possibly *cover* entire QC structure. AlMnPd seems to be "stoichiometric" in sense that these clusters have strict Al–TM order. In AlCuFe case, notion of Al/TM is blurred by Cu atom. Other clusters: **mini-Bergman** is unimportant, chemically irrelevant. PdAl12 icosahedron useful.
- hyperspace description: VALID for Al–Pd(Mn) "skeleton" framework, but INVALID for $MnAl_{10}$ inner-core-pMI ($\sim$20% of the structure!)
- pMI packing adopts **CCT geometry** – the well studied "1/1" approximant is "2/1" CCT tiling. Need to refine/verify D-cell. **Possibly, other kind of the cell might enter the game**
- Energetic stability:
  - important electronic (pseudo) gap formation effect
  - the standard "cluster–level" configurational entropy?
  - huge vibrational/configurational entropy further stabilizing pMI!
  - arrow rules : matching rules? ironically: are these Al atoms that do not have good perp–space representation, responsible for matching rules???

Quasicrystal structure prediction from pair potentials: AlCoNi

AlCoNi system exhibits at least 8 structural modifications of decagonal phase.
Experimental input: in-plane lattice parameter a=2.45A, vertical stacking periodicity c=4.08Å+ composition

Set up a Monte–Carlo with two fundamental degrees of freedom

- reshuffling the "sitelist" via tile flipping
- swapping chemical identities for pairs of sites

M. Mihalkovič et al, "Total-energy-based structure prediction for decagonal Al-Ni-Co", **Phys. Rev. B 65 (2002) 104205**

... predicting QC structures from pair potentials

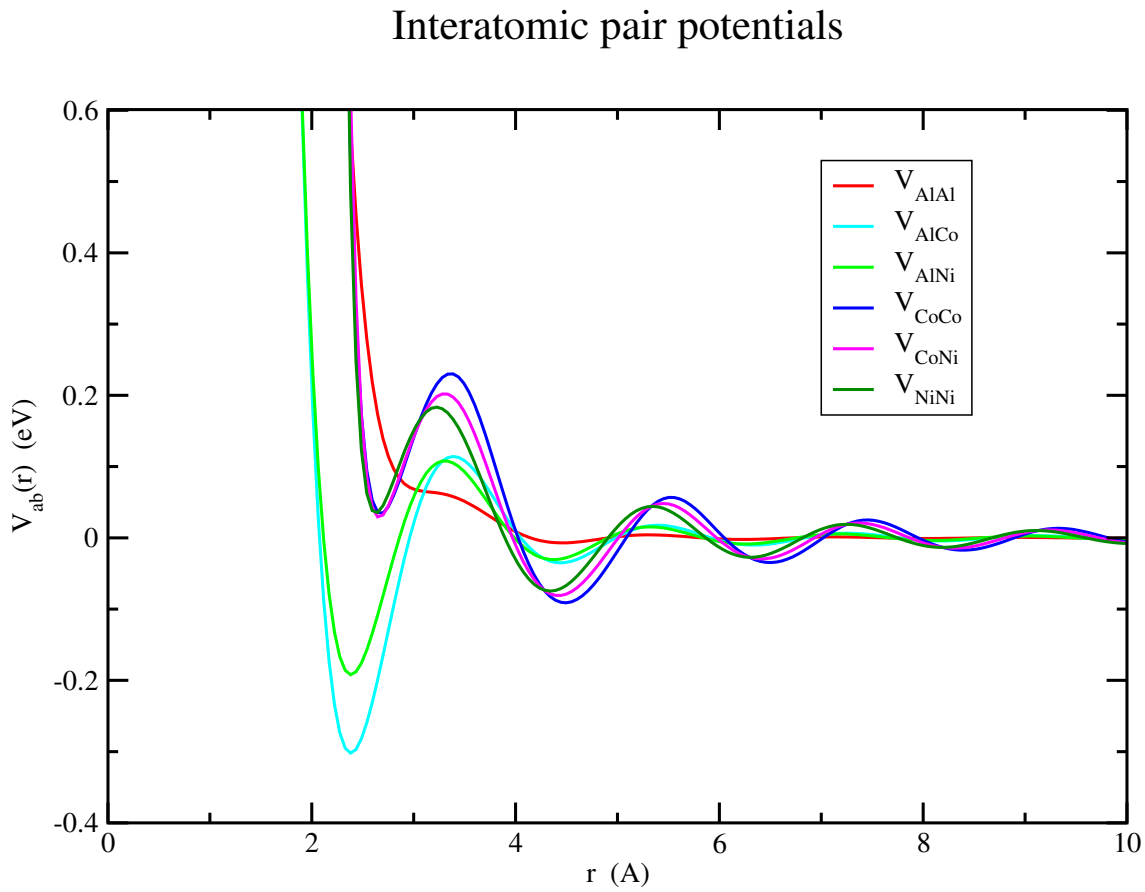

M. Widom, I. Al-Lehyani and J.A. Moriarty, Al-Co and Al-Ni corrected by an additional repulsive term fitted from ab-initio forces, extension to teranry system; "First-principles interatomic potentials for transition-metal aluminides. III. Extension to ternary phase diagrams", **Phys. Rev. B 62 (2000), 3648**

Lattice–gas and tile–reshuffling for Ni-rich d-AlCoNi

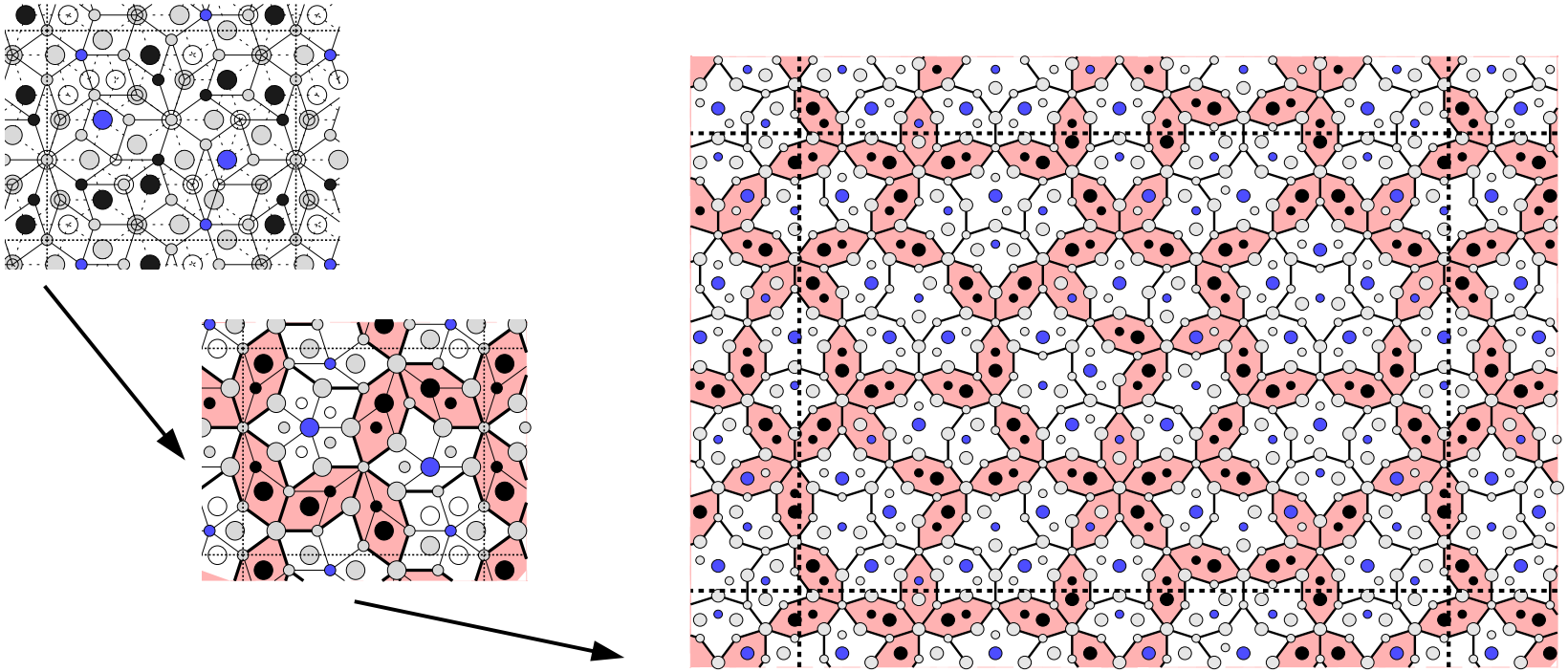

"unilayer simulation": tile-flips and atom swaps $\rightarrow$ HBS tiling

Combined lattice–gas and tile–reshuffling study II: Co-rich d-AlCoNi

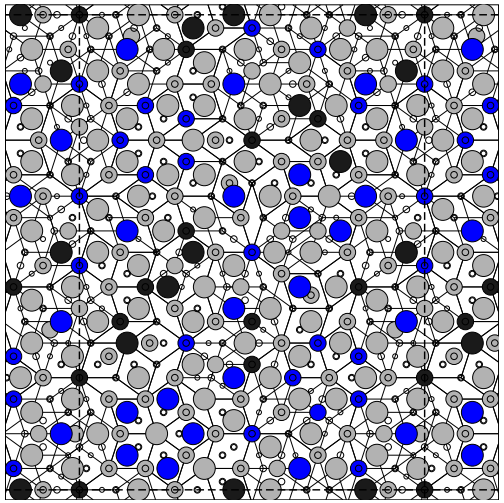

unilayer
unconstrained

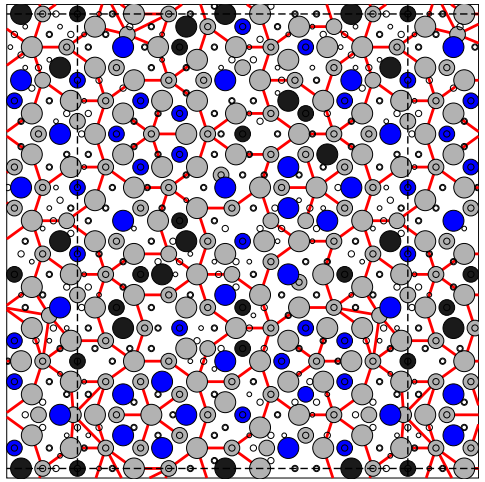

bilayer
unconstrained

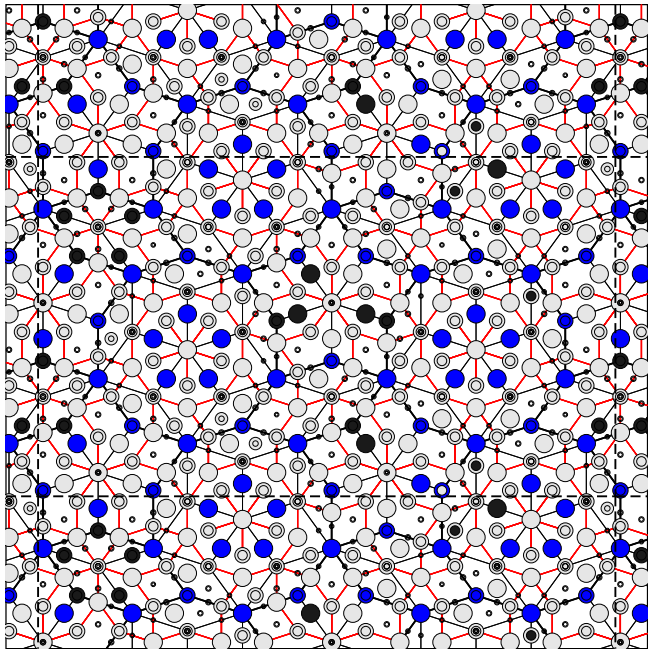

bilayer tile reshuffling

Same procedure applied to Co-rich composition. This time, the dominant motif is **pentagonal cluster** centred by Co–pentagon.

Comparison with W–phase

W–phase: refined by Sugiyama et al (2002)

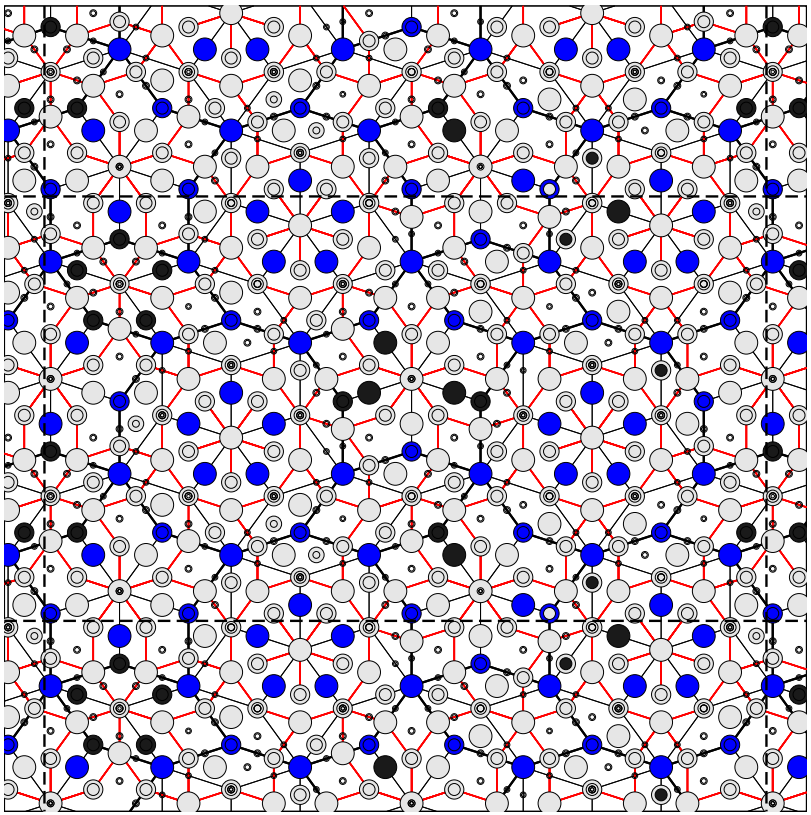

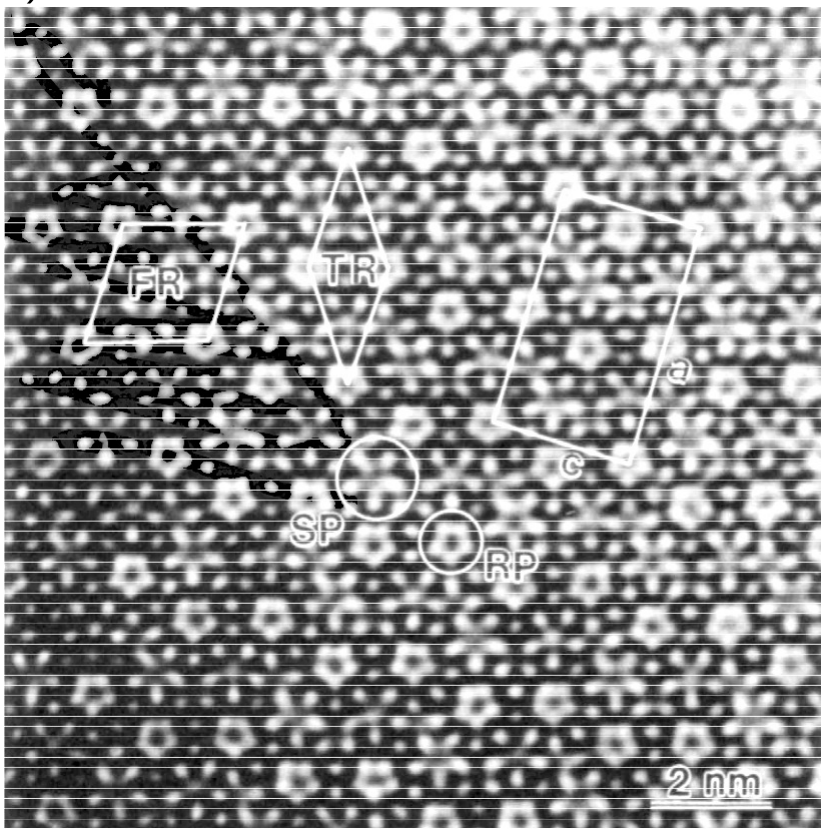

We are surprised by realism with which (i) 4Å–periodic setup and (ii) idealized sitelist in the refinement process reproduce actual atomic structure. However, energies of this series of models are unstable by at least 60 meV/atom, as opposed to refined model of the W itself.

... few years later

Penrose Matching Rules for a Decagonal Quasicrystal from Al-Co Pair Potentials in an almost realistic model with Al4Co stoichiometry Sejoon Lim, Marek Mihalkovič, Christopher L. Henley

constrained–tile-shuffling simulation: Penrose tiling! (except 4 defects/cell forced by periodic b.c.)
Need chem. potential μ_{Al} [tile flip BB $\leftrightarrow$ HS changes 4 Al $\leftrightarrow$ 3 Al)] [provided $-1.55\mathrm{eV} < \mu_{\mathrm{Al}} < -2.05$ eV.]

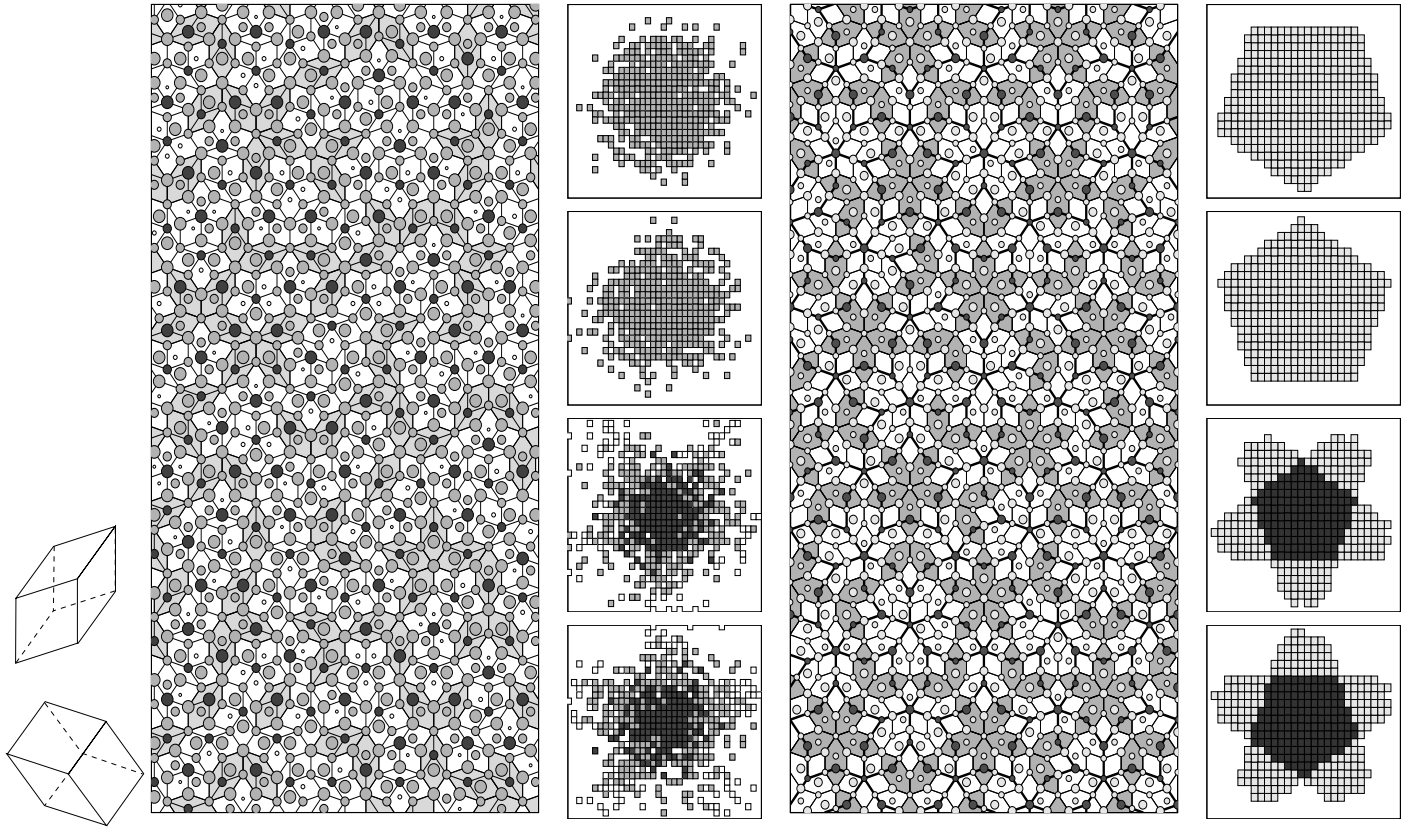

Friedel oscillations!

We will relate these to four aspects of ordering.

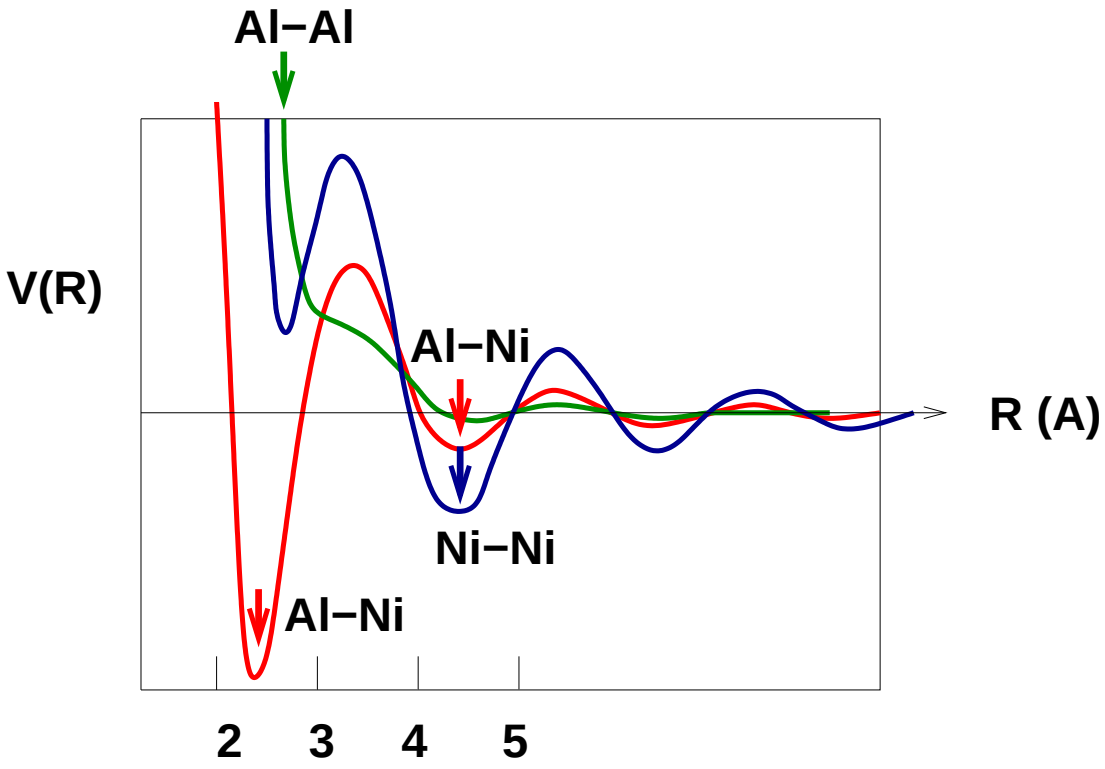

Al-Al, Al-TM (2.5-3Å):
$\Rightarrow$ HBS tiling

TM-TM ($\sim$4.5Å):
$\Rightarrow$ TM supertiling

Al-TM (3.8-4.7Å):
$\Rightarrow$ matching rules

Evolution of order

Aspect (1) Al-Al and Al-TM nearest neighbor
$\Rightarrow$ **HBS tiling**.
Why: $V_{\mathrm{Al-Al}}(R)$ hardcore and strong $V_{\mathrm{Al-TM}}(R)$ attraction near 2.45 Å.

Aspect (2) TM-TM (nearly HBS) supertiling ($\tau a_r \approx 4.0$Å) Due to 2nd neighbor TM-TM.

... diagnostics for matching rules in Al4Co

Diagnostic 2. Vary cutoff radius (or atoms)
(usual was $r_{\rm cut} = 7$Å.)

1 $r_{\rm cut} = 3.5$Å(1st nbr): HBS only

2 $r_{\rm cut} = 5$ Å(2nd well): HBS, Co-Co, m-rule

3 $r_{\rm cut} = 5$ Å, no Al inside Fat:
HBS, Co-Co, V-rule but no Fat-Fat rule

Aspect (3) Fat/Thin matching: "V-rules"

2nd nbr Al-TM ⇒
correct arrows

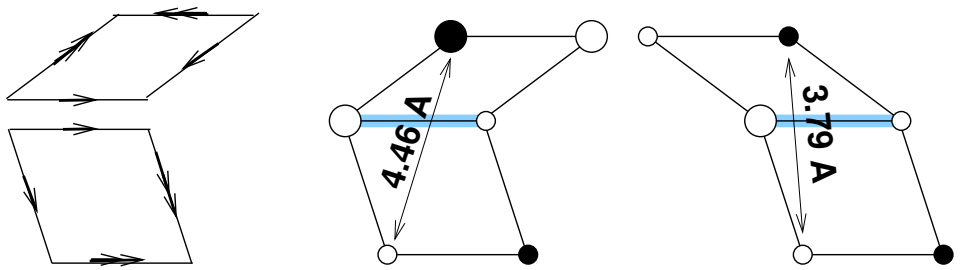

Example
(note Fat Hexagon
around "V")

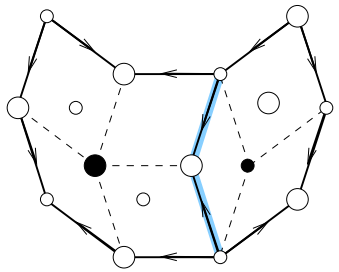

Result is **V-rule**: pair

every Fat-Fat concave corner ↔ every Thin convex corner.

(Possible, iff Penrose number ratio Boat/Star.)

Note no. of 2nd-nbr TM-TM interactions is same in all HBS tilings satisfying the V-rule so **don't** affect matching rules

... whence matching rules?

Aspect (4) Fat/Fat rhombus matching rule: small tile way

Fat rhombus with edges left over from V-rule always contain an internal Al atom. Satisfying the arrows gives one more (favorable) 4.46Å Al-Co bond.

(c).

2nd nbr Al-TM $\Rightarrow$
correct Fat-Fat arrows

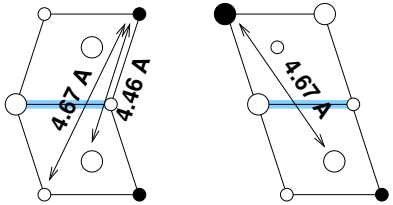

Example

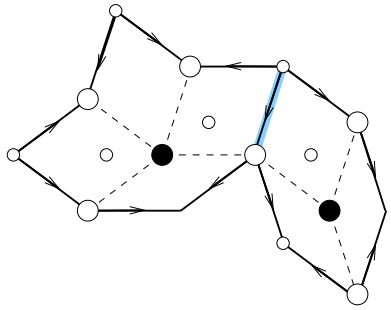

Matching rules in Al3Co...

Rather realistic interactions and a (nearly) realistic composition organized into a Penrose tiling with matching rules. DFT energetics: unstable by 0.1 eV/atom

Due mainly to Al-TM attractive well at $R \approx$4.5Å.

Why it worked?

Different interactions contribute , but favor the **same** result: not "frustrated" [esp. 3rd-neighbor, $R \approx 6.5$Å]

Few environments in Penrose tiling $\Rightarrow$ easy to satisfy all edges.

Penrose case has shortest interaction radius $R_{\min}$ needed to distinguish valid from defective tilings [Levitov, Commun. Math. Phys. 1988; Gähler, Baake, and Schlottmann, PRB 1994]

Crucial to tune the Al content (fortunately it's robust)

Replica exchange method for "cell–constrained melt–quench" (CCMQ) structure prediction

We have found that just by fixing the composition, atomic density, *and the unit cell* of a system to the experimentally known values, we can predict accurately complex **low–temperature** structures with hundred(s) of atoms in the unit cell, without any other structural information. The "cell constraint" seems to limit the ensemble of possible states sufficiently that we can shepherd the system to a low-temperature optimal state using a straightforward "brute-force" technique, in the present case molecular dynamics (MD) melt-quenching.

For very small samples, simple MD is sufficient. For larger samples, we combine "replica exchange" technique with lattice–gas annealing.

Replica exchange: parallel annealing of multiple samples at a *range* of temperatures (20 temperatures 1000K-2500K). Upon completing a *cycle*, attempt to swap samples temperatures, accept with probability $p = exp(\Delta\beta\Delta E)$.

Our typical loop consists of 200 MD steps (at 1-5 fs) and subsequent 100 attempted lattice-gas sweeps of atom pairs.

References for replica exchange: R. H. Swendsen and J. S. Wang, Phys. Rev. Lett. 57, 2607 (1986); M. E. J. Newman and G. T. Barkema, *Monte Carlo methods in statistical physics (Oxford University, New York, 1999)*; P. Ganesh and M. Widom, Phys. Rev. B 77, 014205 (2008)

TEST: known crystal structures

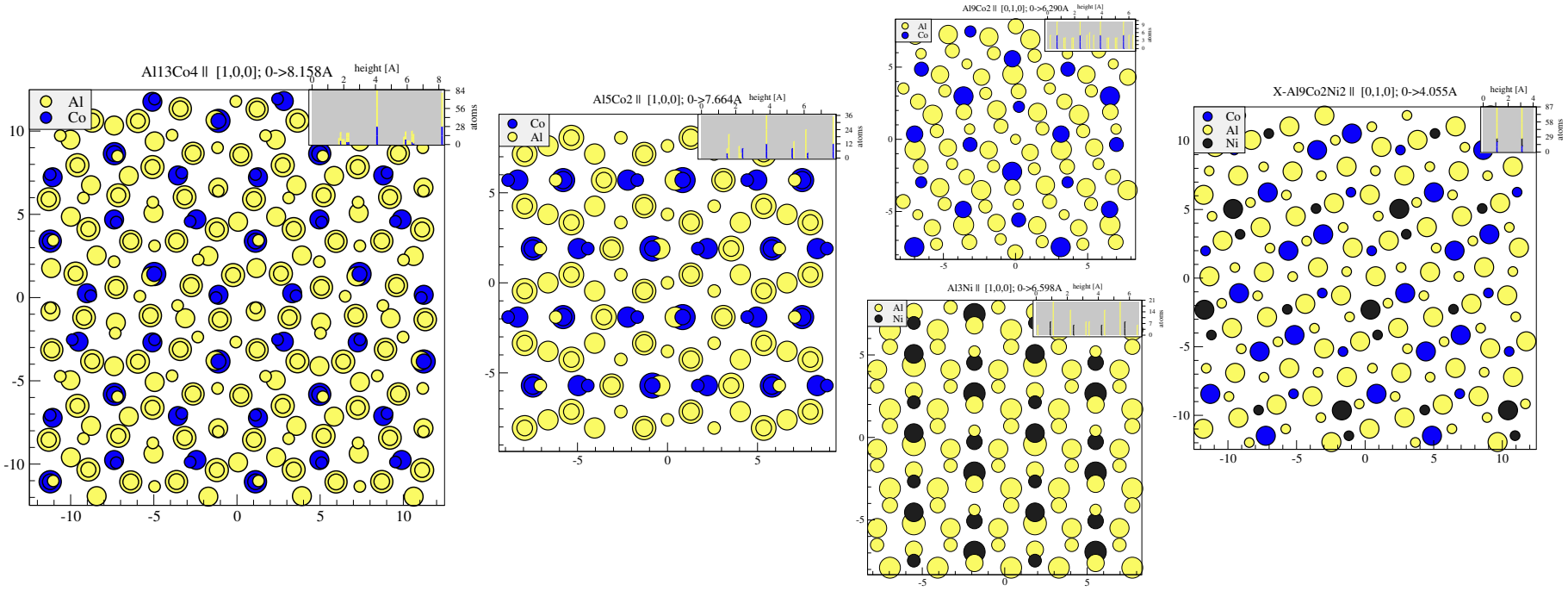

structure	Al9Co2	Al5Co2	Al13Co4	Al3Ni	X-Al9Co2Ni2
atoms/cell	22	28	100†	16	26
loops needed	35	119	2370	10	71

† We used model with 2 vacancies, which is most favourable by ab–initio total energy calculation

The cell–constrained melt–quench (MQ) easily and exactly establishes the known Al–Co, Al–Ni, as well as ternary X-Al9Co2Ni2 phase structures.

CCMQ d-AlCoNi: selecting feasible cell...

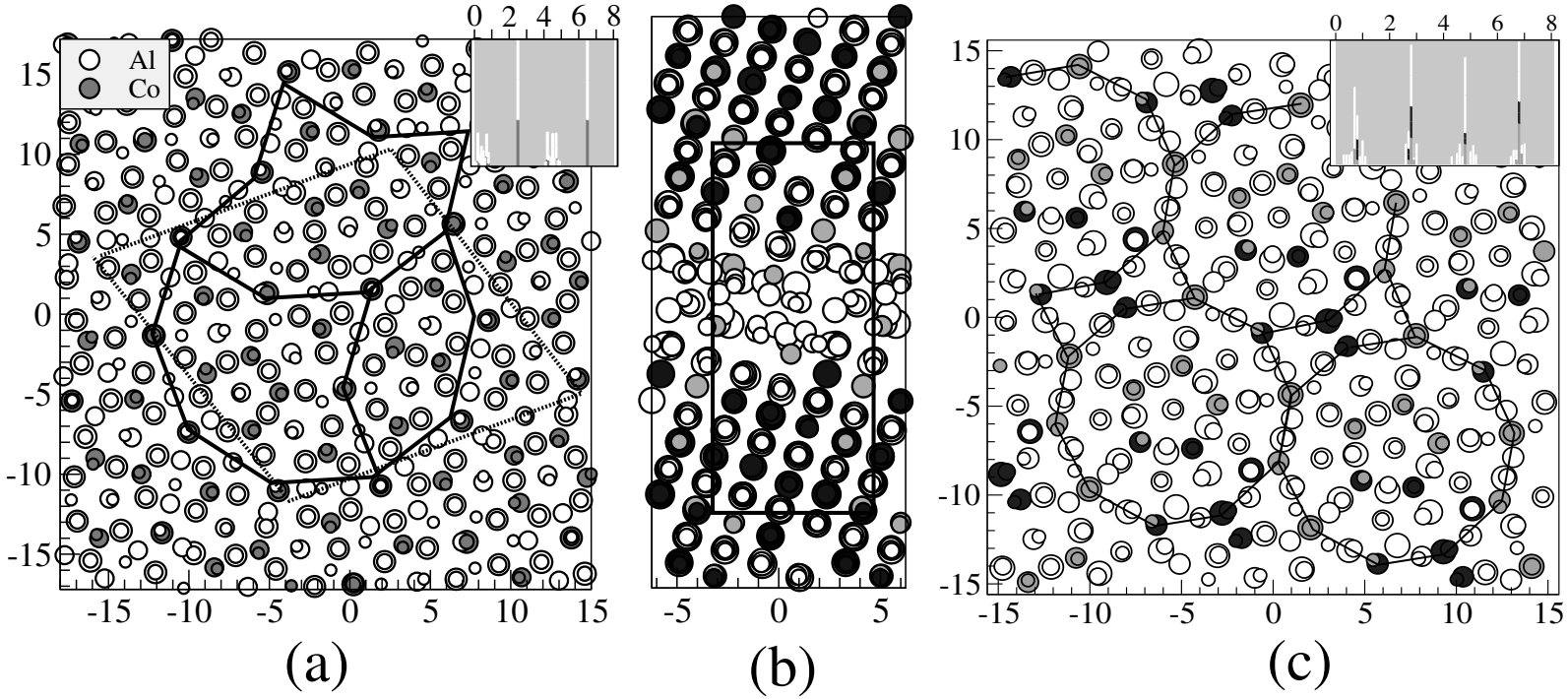

Various outcomes of constrained-cell melt-quench simulation, (a). The "2B+H" unit cell is tractable on the Co-rich side, here $Al_{158}Co_{52}$. The view is along the short (c) axis, except (b); atoms are marked by circles, with larger sizes denoting larger z coordinate. Lines show bonds between atoms in different layers heavy and light for TM-TM and Al-Al, with projected lengths 4.1 ± 0.3Å and 2.6Å, respectively. (b). A B2-like structure found in the same cell for Ni-rich composition $Al_{148}Co_{16}Ni_{41}$ viewed along the (1,1,0) direction) (c axis is horizontal). (c). Co-rich "Co-type" MQ structure $Al_{58}Co_{14}Ni_9$. Composition similar to W-phase (Sugiyama et al).

CCMQ d-AlCoNi, Ni–rich vs Co–rich: WHY??

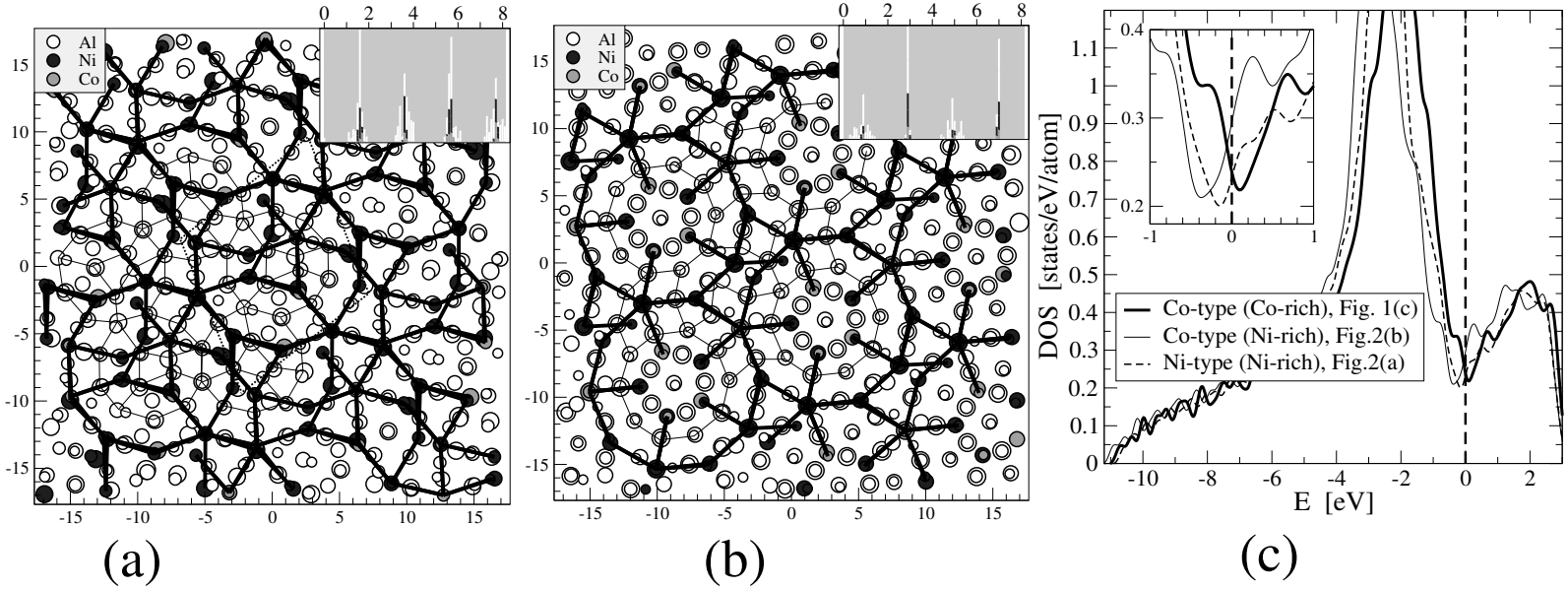

(a,b) Ni-type or Co-type structures emerge in the "Boat" cell, for (respectively) lower density ($Al_{56}Co_6Ni_{16}$) or higher density ($Al_{58}Co_6Ni_{16}$). (c). Electronic density of states (DOS) for Co-type Co-rich ($Al_{58}Co_{14}Ni_9$ in Fig. 1(c)), Co-type Ni-rich (Fig. 2(b)b) and Ni-type Ni-rich (Fig. 2(a)), shifted so that $E_F = 0$.

Cell–constrained melt-quench (CCMQ) unbiased test: MgPd system

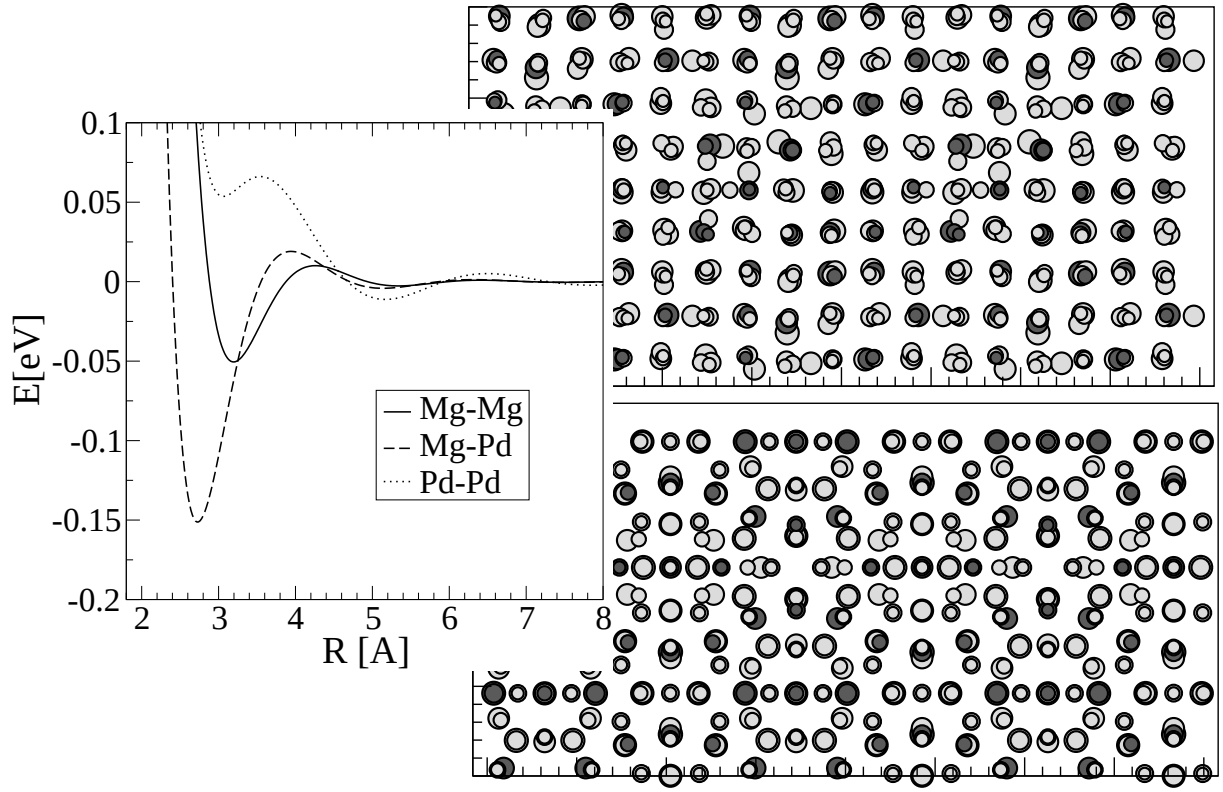

We start without apriori knowledge of ANY MgPd structure - our samples for pair potential fit are taken from **liquid** state at several compositions. The pair potential is then used in CCMC simulation.

Ab–initio comparison with diffraction data

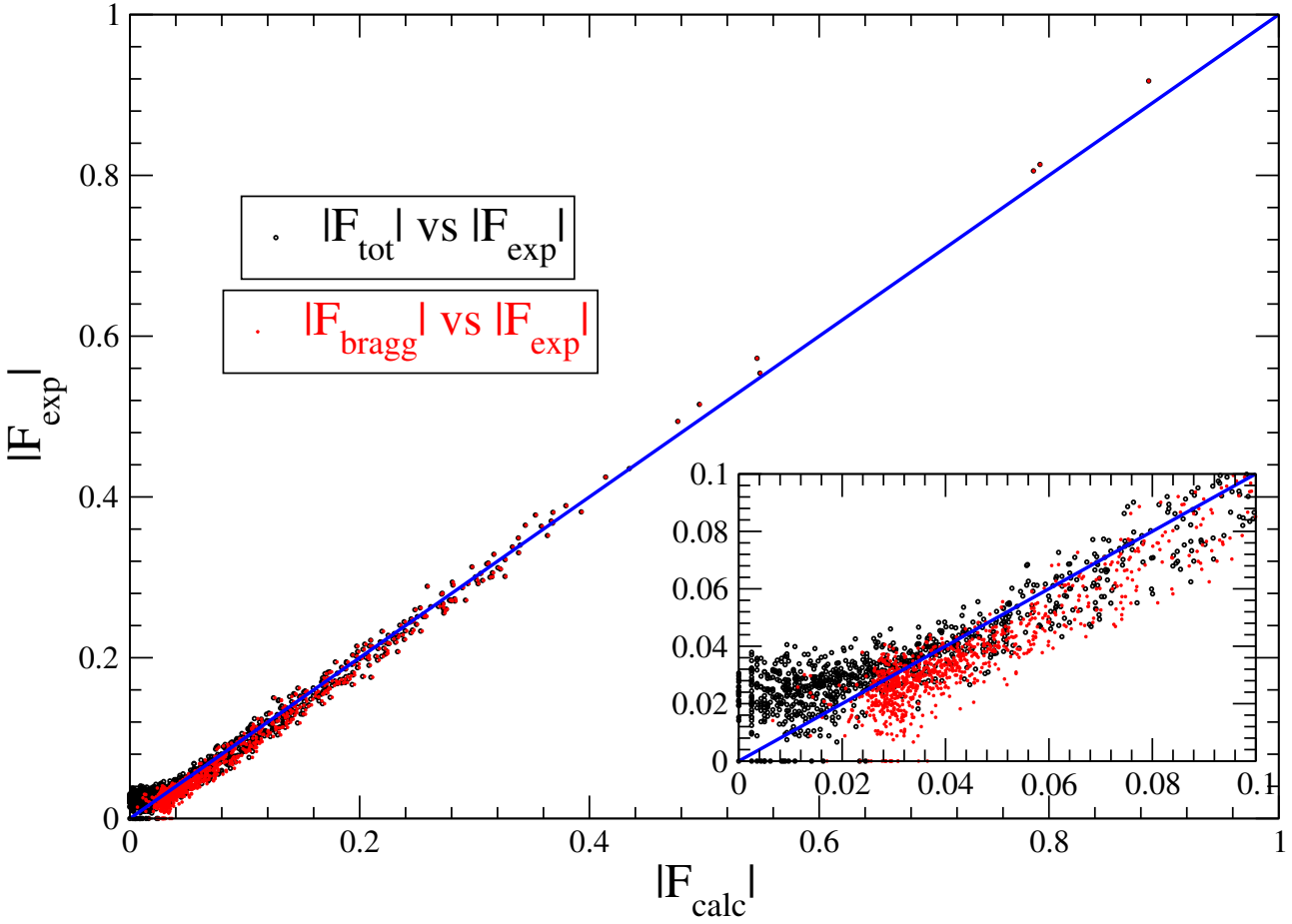

F_{tot} is time average over intensities, F_{bragg} is time-average over Fourier **amplitudes**, in the course of MD run (take care about drift due to finite size!!). (So we have immediate access to the diffuse part: $I_{diffuse}$=$I_{tot} - I_{bragg}$).

Application: systems with mixed/parital occupancies, simulation base on MC rather than MD (or combination);
purpose: decouple erroneous mixing of Debye–Waller factor with mixed/fractiopnal ocupancies.

Cell–constrained melt-quench: atomic structure of 2/1-1/0-1/0 approximant AlCuSc

Ishimasa, Hirao, Honma – 2008–2010

1. composition $Al_{36.4}Cu_{48.1}Sc_{15.5}$

2. orthorhombic centred cell, 8.34×22.02×8.31 Å

... AlCuSc approximant by melt quenching...

1. substitution (Al,Cu)$\rightarrow$Zn
2. CCMQ simulation for 54 atoms. Needed to tune potentials to avoid formation of disordered B.C.C.

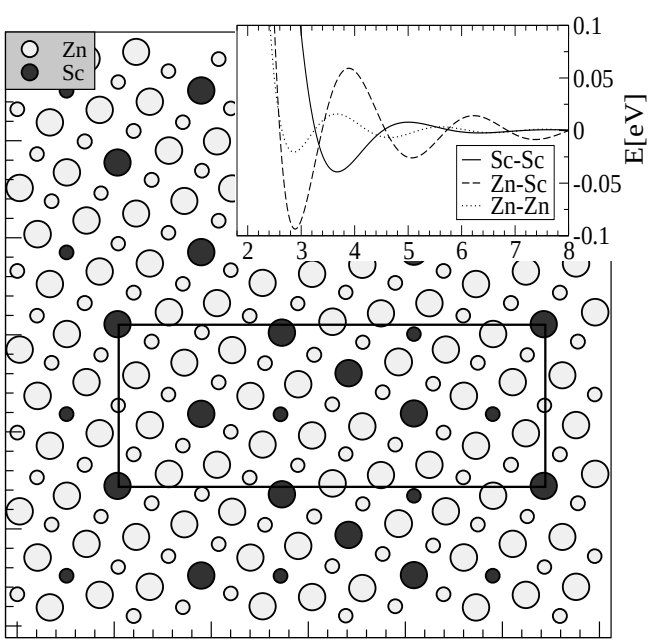

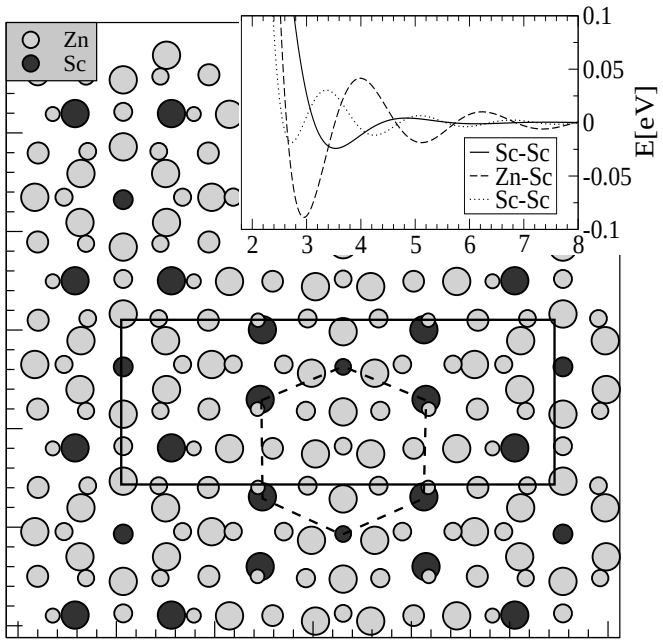

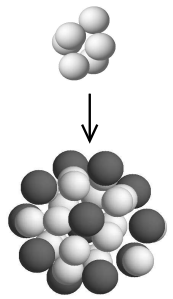

... AlCuSc approximant by melt quenching.

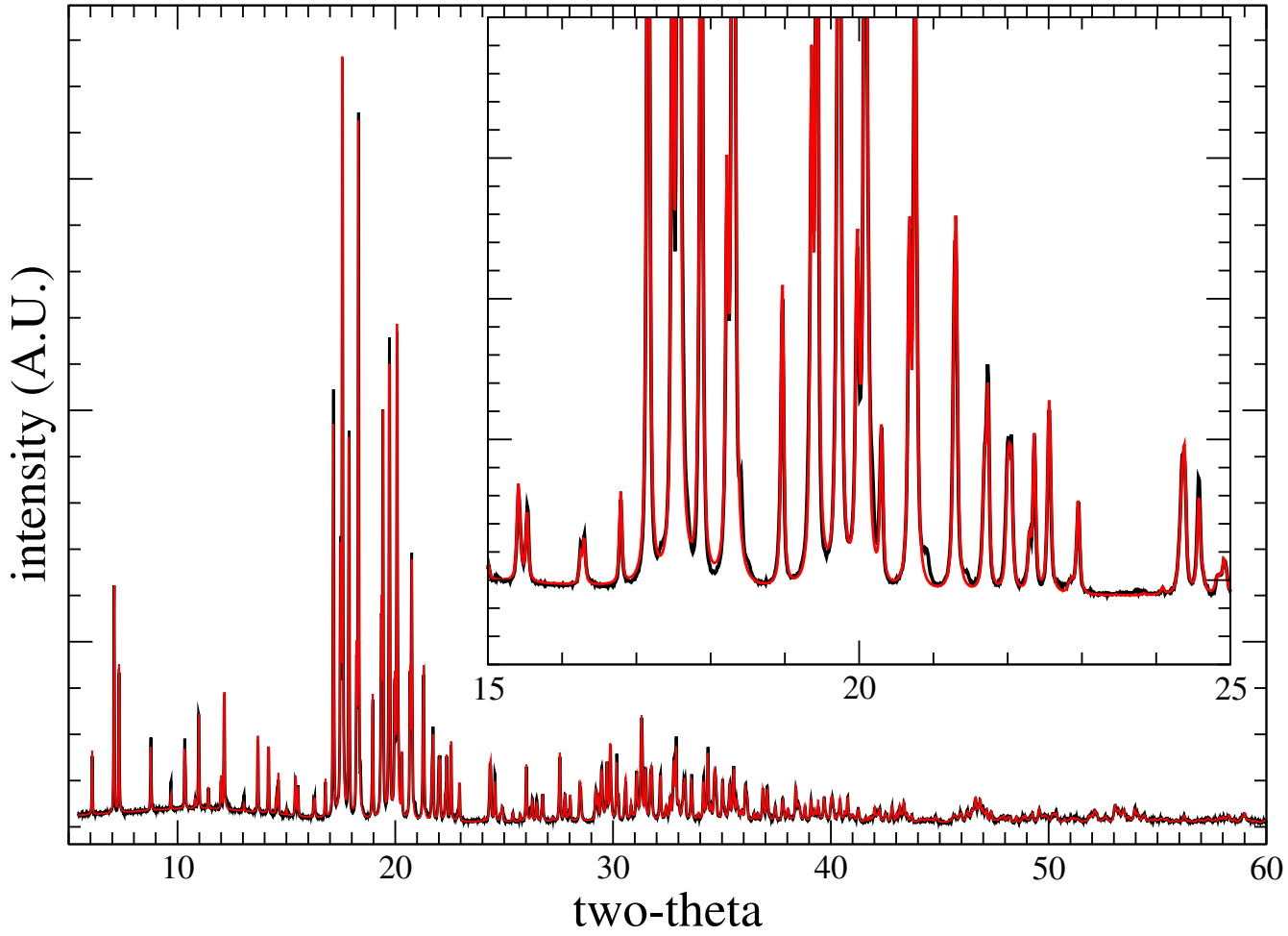

... Final structure solution, comparison with experimental powder Xray data (black:measured; red:model, Rietveld refined). A single modification of the initial structure was 1/2 occupancy of one Wyckoff position

... decagonal clathrate

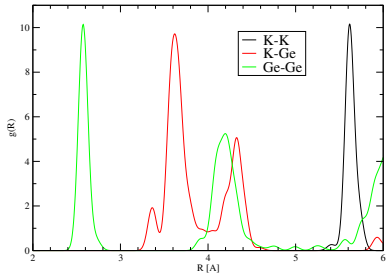

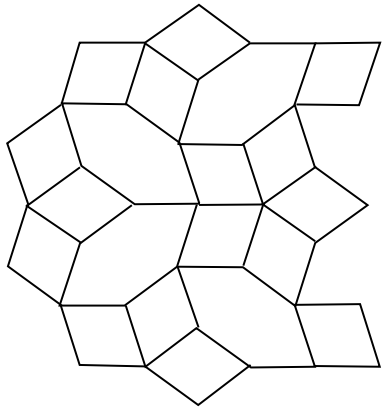

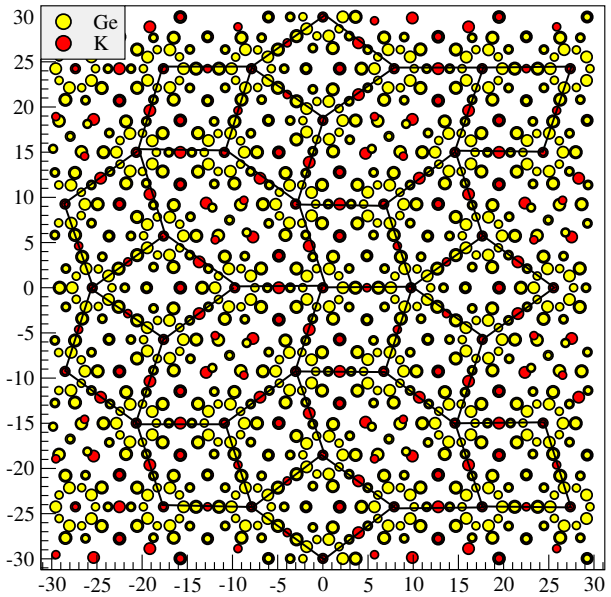

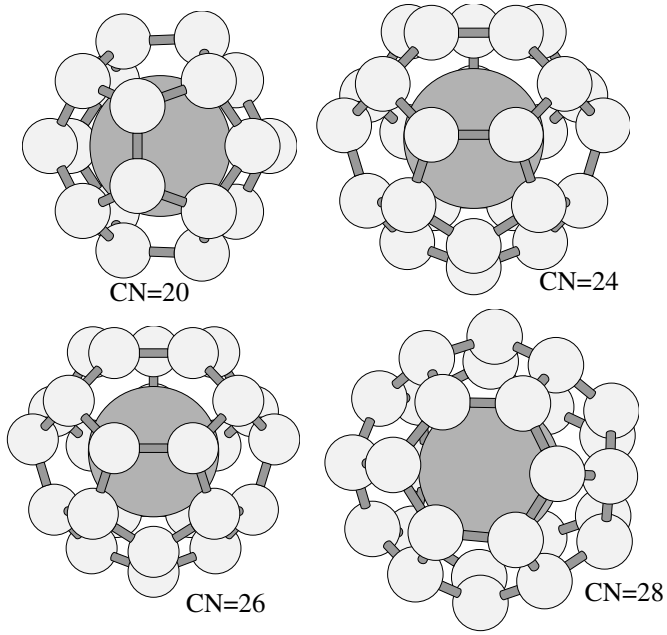

Clathrate structures are DUAL to Frank–Kasper polyhedra (O'Keeffe, G. B. Adams, O. F. Sankey, Phil. Mag. 78, p. 21 (1998)): any proper Frank–Kasper structure has related "intergrowth" clathrate structure. Idea tested on decagonal Frank–Kasper approximants, **works for Ge–K system**, in which large approximant are only 1-4 meV/atom unstable!

The structure shown is orthorhombic centred $Ge_{636}K_{112}$, pearson symbol oA748, a=11.2Å, b=148.5Å, c=35.3Å. Very likely, stable decagonal clathrates could be obtained by having different types of (large) guest atoms.

Hf4Mg16Zn80

Discovered by Gomez et al, 2008. Hf atom is "Large", ∼80% Zn content is intriguing: like in other cases (ScZn6, Mg2Zn11) we expect effect

Table shows fractionally occupied Wyckoff sites (sp.grp. $Pm\bar{3}$.

Mg4	8i	0.898*Mg 0.102*Hf
Zn8	12k	0.967*Zn 0.033*Mg
Zn10	6f	0.833*Zn 0.167*Mg
Zn14	6h	0.5*Zn
Zn15	12k	0.5*Zn
Mg12	8i	0.588*Mg 0.412*Zn
Zn17	24l	0.077*Zn
Zn18	12k	0.368*Zn
Zn19	12k	0.108*Zn

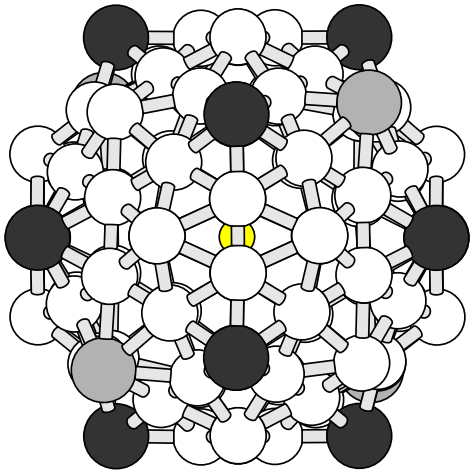

CORNER: Bergman cluster

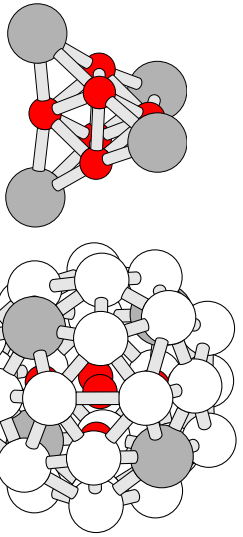

BodyCenter

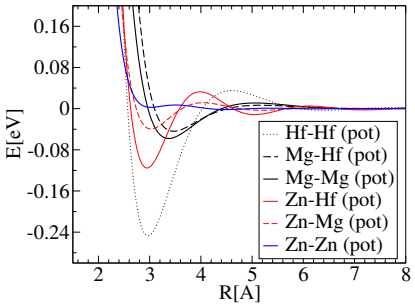

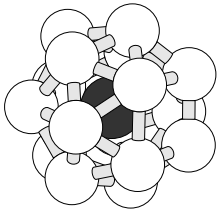

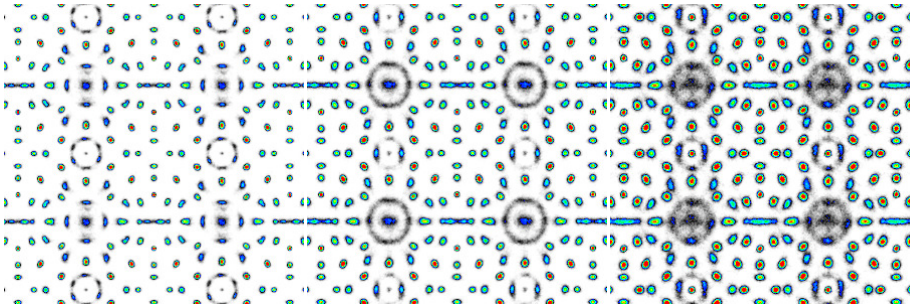

...Hf4Mg16Zn80 : results

struc	ΔE meV/at.	ΔH meV/at.	x(Hf) %	x(Mg) %	x(Zn) %	note
CaCd6.cI208/ch1	-1.1	-110.4	7.1	7.1	85.7	UNKNOWN
HfMgZn.cP208/30-127	0.2	-109.6	3.8	15.3	80.9	octa.
HfMgZn.cP208-Zn-at-Mg12	4.3	-95.8	3.8	12.7	83.4	octa.
HfMgZn.cP208-Zn-at-Mg12	7.0	-92.0	3.8	12.6	83.6	double-tetra.
HfMgZn.cP208/30-129	7.2	-101.4	3.8	15.1	81.1	double-tetra.
HfMgZn.cP208-Mg-at-Mg12	16.2	-99.8	3.8	17.0	79.2	
MgZn2.hP12/ch1	19.5	-139.2	8.3	25.0	66.7	
HfZn2.cF24	97.7	-76.9	16.7	16.7	66.7	

Note: Laves phases are stable in both binaries, but UNSTABLE in ternary!
Note: The phase in unstable in Mg–Zn binary by as much as 33 meV/atom!
$\rightarrow$ Mg is VERY uncomfortable inside pure-Zn-Friauf! (needs Mg nearest neighb.)